

Up-Down Asymmetry in Inelastic Electron-Polarized-Proton Scattering*

ROBERT N. CAHN†

Department of Physics and Lawrence Radiation Laboratory, University of California, Berkeley, California 94720

AND

Y. S. TSAI

Stanford Linear Accelerator Center, Stanford University, Stanford, California 94305

(Received 2 April 1970)

We have investigated the up-down asymmetry in inelastic electron scattering from polarized protons. It is shown that the contributions from (possible) T violation and α^3 effects can be separated experimentally. We have demonstrated that the contribution of bremsstrahlung emission to the asymmetry is negligible. An expression for the two-photon-exchange contribution is obtained, assuming a proton intermediate state and N^* (1238) final state. The expression has been evaluated numerically and found to be one order of magnitude smaller than the observed asymmetry. A general formalism for calculating the up-down asymmetry is presented and its physical significance discussed. The relation between T violation and the measurement of the asymmetry given by Christ and Lee is sharpened and the experimental results of the Berkeley-SLAC collaboration are discussed.

I. INTRODUCTION

INELASTIC electron scattering from a polarized proton was suggested by Christ and Lee¹ to test time-reversal invariance in electromagnetic interactions involving hadrons. The experiment was carried out at CEA by Chen *et al.*,² and more recently at SLAC by a Berkeley-SLAC collaboration,³ and the results of the latter show some up-down asymmetry as shown in Fig. 1. Christ and Lee¹ showed that in the α^2 cross section the up-down asymmetry should be zero if parity conservation and time-reversal invariance hold. It is obvious that if the up-down asymmetry is due to a violation of time-reversal invariance, the asymmetry should have the same sign whether the incident particle is an electron or a positron, because in the lowest-order Born approximation the cross section is proportional to the square of the charge of the electron. On the other hand, the α^3 cross section has two parts⁴: one which changes

sign and one which does not, when e^- is replaced by e^+ . In Sec. II we show that only the part which changes sign contributes to the up-down asymmetry if T and P invariances hold. Therefore, if T invariance holds, the experimental points for e^+p and e^-p in Fig. 1 should be symmetric (up to α^3 in cross section) with respect to the line representing no up-down asymmetry. This simple consideration shows that up to α^3 in cross section the effects of T violation and α^3 cross sections can be separated out experimentally and are given, respectively, by

$$A(T \text{ violation}) = \frac{\sigma_{e^- \uparrow} - \sigma_{e^- \downarrow} + \sigma_{e^+ \uparrow} - \sigma_{e^+ \downarrow}}{\sigma_{e^- \uparrow} + \sigma_{e^- \downarrow} + \sigma_{e^+ \uparrow} + \sigma_{e^+ \downarrow}} \quad (1.1)$$

and

$$A(\alpha^3) = \frac{\sigma_{e^- \uparrow} - \sigma_{e^- \downarrow} - \sigma_{e^+ \uparrow} + \sigma_{e^+ \downarrow}}{\sigma_{e^- \uparrow} + \sigma_{e^- \downarrow} + \sigma_{e^+ \uparrow} + \sigma_{e^+ \downarrow}}. \quad (1.2)$$

Hence, in order to test the T invariance, it is not neces-

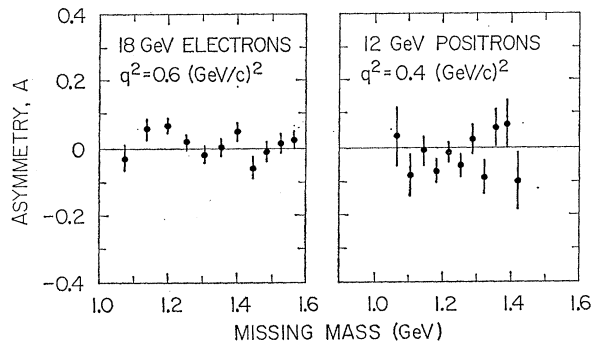


FIG. 1. Experimental results of Rock (Ref. 3).

* Work supported by the U. S. Atomic Energy Commission.

† National Science Foundation Predoctoral Fellow.

¹ N. Christ and T. D. Lee, *Phys. Rev.* **143**, 1310 (1966).

² J. R. Chen *et al.*, *Phys. Rev. Letters* **21**, 1279 (1968); J. A. Appel *et al.*, *Phys. Rev. D* **1**, 1285 (1970).

³ S. Rock *et al.*, *Phys. Rev. Letters* **24**, 748 (1970).

⁴ Y. S. Tsai, *Phys. Rev.* **122**, 1898 (1961).

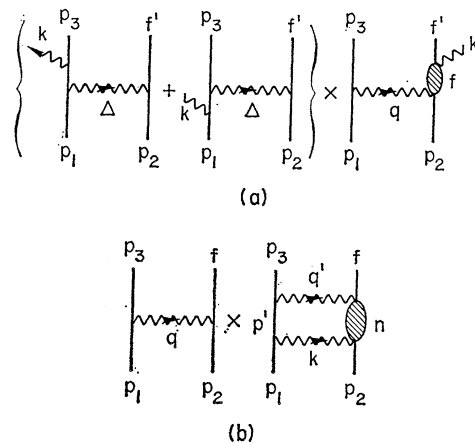


FIG. 2. Two classes of Feynman diagrams which contribute to the up-down asymmetry. f , f' , and n are arbitrary states. p_2 represents the polarized target proton. p_1 and p_3 are incident and outgoing electrons, respectively.

sary to calculate the up-down asymmetry due to α^3 cross sections.

Nevertheless, we have investigated the part of the α^3 cross section which gives the up-down asymmetry for its own interest.⁵ From the discussion in Sec. II, the most general classes of α^3 diagrams contributing to the up-down asymmetry are as shown in Figs. 2(a) and 2(b). Figure 1 shows that no statistically significant evidence of T violation was found. The positron and electron data were taken at different incident energies so no meaningful separation of two effects is possible from the data.⁶ However, if we ignore the possibility of T violation, the electron data do show some evidence of α^3 effect between one-pion threshold and two-pion threshold. It happens that the nature of the final states in this kinematical region is better known than in other regions from other experiments. Therefore, we shall concentrate our discussion in this region. In this kinematical region, f' in Fig. 2(a) is either p or $N+\pi$, and f in Fig. 2(b) is $N+\pi$.

The purpose of this paper is the following: (1) to develop a general formalism for calculating the up-down asymmetry; (2) by assuming some simple intermediate and final states for Figs. 2(a) and 2(b), and actually calculating their contributions to the asymmetry, to learn not only many of the salient features of the problem, but also to obtain a rough order of magnitude of the asymmetry; (3) to investigate what physics one can learn from this kind of experiment in general.

In Sec. II, we first generalize the theorem given by Christ and Lee to include the higher-order electromagnetic effects and to show that only the imaginary parts of two classes of diagrams shown in Figs. 2(a) and 2(b) contribute to the up-down asymmetry if T and P invariances hold. From Figs. 2(a) and 2(b), it is obvious that phases of the final states always get canceled out; hence one can always use the convention that the Feynman diagrams on the left of each figure are real, and an imaginary part can occur only when all the particles in the intermediate states of the right-hand side of each figure are on the mass shell.

We also show that $A(T$ violation) is proportional to the interference between the normal current j_i^n and the abnormal current j_i^a , where $PTj_i^n(PT)^{-1}=j_i^n$ and $PTj_i^a(PT)^{-1}=-j_i^a$. This is very similar to the effect of parity nonconservation in weak interactions where

⁵ A. O. Barut and C. Fronsdal, Phys. Rev. **120**, 1871 (1960); F. Guerin and C. A. Pickett, Nuovo Cimento **32**, 971 (1964).

⁶ In the kinematical region between the one-pion threshold and the peak of the 3-3 resonance, the main contributions to the cross sections are from the p -wave 3-3 resonance and the s -wave pion production. The latter contributes about 10% to the cross section at the peak. However, the s -wave part can be roughly reproduced by Born diagrams which are real; hence we do not expect the s -wave part to contribute to the up-down asymmetry in Fig. 2(a). In Fig. 2(b), the up-down asymmetry is independent of the phase of the final state; hence the argument given above does not apply. In a more complete treatment of the problem, the s -wave part has to be included in both the denominator and the numerator of A_i in Eq. (4.13).

the observable effects show only in the interference terms between the vector and axial-vector currents.

In Sec. III, we treat the class of diagrams represented in Fig. 2(a). We find that these diagrams contribute a negligible amount to the up-down asymmetry compared with the experiment. In Sec. IV, we treat Fig. 2(b) assuming that the final state is an $N^*(1238)$ and the intermediate state is a proton. For these particular final and intermediate states, the contribution to the up-down asymmetry is found to be roughly $\frac{1}{10}$ of the maximum observed asymmetry. In Sec. V, we sharpen the Christ-Lee theorem and show that the measurement of $A(T$ violation) gives a lower bound for the ratio of the magnitude of the abnormal current to that of the normal current. It is pointed out that unless there are some conspiring cancellations among the products of the matrix elements of j_x^a and j_x^n and those of j_z^a and j_z^n at all energies and angles, the smallness of the asymmetry found by Rock *et al.*³ indicates the smallness of j^a compared with j^n . Hence, it is unlikely that the apparent CP violation in the decay $K_2 \rightarrow 2\pi$ is due to the T violation in the electromagnetic interaction of hadrons. We also give a general formula for calculating $A(\alpha^3)$ for arbitrary final and intermediate states in terms of a product of three currents. Possible refinements of our calculation of $A(\alpha^3)$ are discussed. The relations between the two-photon exchange which appears in the calculation of $A(\alpha^3)$ and other observable two-photon interaction phenomena are discussed. Appendix A gives an alternative derivation of some of the results of Sec. II using T and P invariances and unitarity of the S matrix. Appendix B gives an example of how to use Cutkosky's rule to obtain the imaginary part of a two-photon-exchange diagram. Appendix C shows why the infrared divergent parts of Figs. 2(a) and 2(b) do not contribute to the up-down asymmetry. In Appendix D we show that owing to the current conservation, no singularity is induced by ignoring the mass of the electron in calculating the up-down asymmetry, and hence no terms such as $\ln(s/m^2)$ or $\ln(-t/m^2)$ occur in the up-down asymmetry.

II. PRELIMINARY CONSIDERATIONS

In this section we summarize all those observations which can be made without lengthy calculations. The incident and outgoing electrons are labeled p_1 and p_3 , respectively, and the target proton is denoted by p_2 . s is the polarization vector of the target proton.

A. Since we are dealing with an experiment which detects only one final electron, we have only four independent vectors p_1 , p_2 , p_3 , and s to construct an invariant representing the asymmetry. This invariant must be linear in s . Since s is a pseudovector, Lorentz invariance and parity conservation demand that the asymmetry be proportional to

$$\epsilon_{\alpha\beta\gamma\delta} p_1^\alpha p_3^\beta p_2^\gamma s^\delta = M [(\mathbf{p}_1 \times \mathbf{p}_3) \cdot \mathbf{s}]_{\text{lab}}. \quad (2.1)$$

Thus as long as only one final electron is detected, only the component of the polarization vector perpendicular to the scattering plane can enter into the expression for the asymmetry. This is true no matter what the final states of other unobserved particles are, and true to all orders in strong and electromagnetic interactions. Let us denote the initial proton state by $|p_2\uparrow\rangle$ if the

spin of p_2 is parallel to $\mathbf{p}_1 \times \mathbf{p}_3$ and $|p_2\downarrow\rangle$ if it is antiparallel to $\mathbf{p}_1 \times \mathbf{p}_3$. Let us define a coordinate system in the laboratory frame as shown in Fig. 3. In the laboratory system, s can be written as

$$s = (s_0, s_x, s_y, s_z) = (0, 0, S, 0), \quad (2.2)$$

where⁷

$$S = \frac{\text{number of protons with spin up} - \text{number of protons with spin down}}{\text{number of protons with spin up} + \text{number of protons with spin down}}. \quad (2.3)$$

Later we shall use the rest frame of the final undetected particle or particles (rest frame of N^* , hereafter referred to as the R frame) to perform the spin sum and the c.m. system ($\mathbf{p}_1 + \mathbf{p}_2 = 0$, hereafter referred to as the C frame) to perform the integration in the two-photon-exchange diagram. Since both the C frame and the R frame are obtained from the laboratory system (hereafter denoted as the L frame) by Lorentz transformations in the scattering plane (the xz plane), the components of s given by Eq. (2.2) are unchanged by the Lorentz transformations, i.e., s has only the y component in L , C , and R frames.

B. We show that if T invariance holds, those terms in the α^3 cross sections which do not change sign when e^- is replaced by e^+ will not contribute to the asymmetry. These terms can be classified into three categories: (1) interference between the lowest-order Born term (e^2) and the next-order terms (e^4) which still contain only one photon exchange—such as vertex corrections, self-energy diagrams, and the vacuum polarization diagram; (2) squares of bremsstrahlung diagrams all of which contain one real photon emission from electron lines only; (3) squares of bremsstrahlung diagrams all of which contain one real photon emission from hadron lines only. The e^4 terms in the category (1) have the same structure as the e^2 term but with different form factors; hence, from the Christ-Lee theorem they should not contribute to the asymmetry if T invariance holds. The Christ-Lee theorem also applies to category (3). Hence we need to consider only category (2). However, we observe that for all three categories (a) only one virtual photon is exchanged between the electron cur-

rent and the hadron current, and (b) there is no interference between photons emitted by electrons and those emitted by hadrons. We prove in the following that no asymmetry can be produced under these two assumptions. Our proof can be regarded as a generalization of the Christ-Lee theorem. With these two assumptions, the asymmetry can be written as

$$A = \sigma(\uparrow) - \sigma(\downarrow) \propto \int d^4\Delta L^{\mu\nu}(1/\Delta^4) B_{\mu\nu}, \quad (2.4)$$

where Δ is the four-momentum of the photon exchanged between the electron system and the hadron system (note that Δ is not necessarily equal to $q = p_1 - p_3$ because we are allowing the possibility of bremsstrahlung emission by electrons). $B_{\mu\nu}$ is the second-rank tensor representing the product of two hadron sides of the matrix elements:

$$B_{\mu\nu} = \sum_f [\langle p_2\uparrow | j_\mu | f \rangle \langle f | j_\nu | p_2\uparrow \rangle - \langle p_2\downarrow | j_\mu | f \rangle \langle f | j_\nu | p_2\downarrow \rangle] \delta^4(\Delta + p_2 - p_f), \quad (2.5)$$

where the final state f is allowed to have any number of photons emitted by hadrons in addition to the hadrons. $L^{\mu\nu}$ is a similar tensor representing the product of two lepton sides of the matrix elements, except that the sign between the two terms in Eq. (2.5) should be changed to plus because the incident electron is not polarized. Current conservation requires $\Delta^\mu B_{\mu\nu} = \Delta^\nu B_{\mu\nu} = 0$; therefore, we need to consider only the space components B_{ij} of $B_{\mu\nu}$ with $i, j = 1, 2, 3$, the fourth component being determined by the other three. Hermiticity of the electromagnetic current j_i requires

$$B_{ij}^* = B_{ji}. \quad (2.6)$$

On the other hand, taking the complex conjugate of Eq. (2.5) directly and using the antiunitarity of the

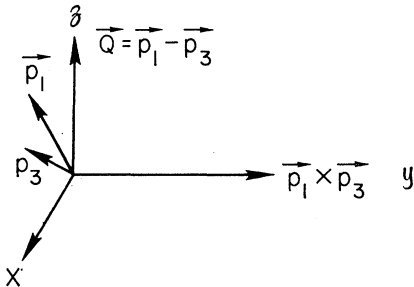


FIG. 3. Coordinate system used in the calculation.

⁷ In the calculation of the asymmetry $d\sigma(\uparrow) - d\sigma(\downarrow)$, s is set equal to $(0, 0, 1, 0)$ and hence

$$\gamma_5 s = \begin{bmatrix} \sigma_y & 0 \\ 0 & -\sigma_y \end{bmatrix}.$$

$X=PT$ operator, we obtain

$$B_{ij}^* = \sum_f [\langle X(p_2\uparrow) | X j_i X^{-1} | X f \rangle \langle X f | X j_j X^{-1} | X(p_2\uparrow) \rangle - \langle X(p_2\downarrow) | X j_i X^{-1} | X f \rangle \langle X f | X j_j X^{-1} | X(p_2\downarrow) \rangle] \times \delta^4(\Delta + p_2 - p_f). \quad (2.7)$$

In the laboratory system p_2 is at rest, and our states $|p_2\uparrow\rangle$ and $|p_2\downarrow\rangle$ are eigenfunctions of the angular momentum operator J_y with eigenvalues $\frac{1}{2}$ and $-\frac{1}{2}$, respectively. Using Wigner's convention, we have

$$X | p_2\downarrow \rangle = - | p_2\uparrow \rangle \quad (2.8)$$

and

$$X | p_2\uparrow \rangle = + | p_2\downarrow \rangle. \quad (2.9)$$

If PT invariance holds, the current operator j_i satisfies

$$X j_i X^{-1} = j_i. \quad (2.10)$$

Obviously we have

$$\sum_f |X f\rangle \langle X f| \delta^4(\Delta + p_2 - p_f) = \sum_f |f\rangle \langle f| \delta^4(\Delta + p_2 - p_f). \quad (2.11)$$

Substituting Eqs. (2.8)–(2.11) into Eq. (2.7), we obtain

$$B_{ij}^* = -B_{ij}. \quad (2.12)$$

Comparing Eq. (2.6) with Eq. (2.12), we conclude that

$$B_{ij} = -B_{ji}. \quad (2.13)$$

Using a similar argument we obtain $L^{ij} = L^{ji}$, hence $L^{\mu\nu} B_{\mu\nu} = 0$. Since all three categories of terms can be written in the form of Eqs. (2.4) and (2.5), we have proved our assertion. In other words, the terms in the α^3 cross section which contribute to the up-down asymmetry are (a) interference between the lowest Born approximation and the two-photon-exchange diagram, and (b) interference between bremsstrahlung originating with the electron and that originating with the hadron. In both of these cases the cross section is proportional to the cube of the charge of the electron. Hence when e^- is replaced by e^+ , this asymmetry changes sign.

C. We show that if the up-down asymmetry is produced by an interference between two diagrams T_1 and T_2 , then only the imaginary part of $T_1^\dagger T_2$ contributes to the asymmetry. By definition the asymmetry produced by the interference between T_1 and T_2 is proportional to

$$A = \sum_{\substack{\text{spin of} \\ \text{all particles}}} \text{Tr} \gamma_5 \mathbf{s} (T_1^\dagger T_2 + T_2^\dagger T_1), \quad (2.14)$$

where $\mathbf{s} \equiv \gamma^\mu s_\mu$, and $\sum_{\text{spin}} T_1^\dagger T_2$ can in general be expressed as a sum of terms each of which is expressible as a product of γ matrices and an invariant function.

Let us write, therefore,

$$\sum_{\text{spin}} \text{Tr} \gamma_5 \mathbf{s} T_1^\dagger T_2 = \sum_i \text{Tr} \gamma_5 \mathbf{s} \Gamma_i F_i, \quad (2.15)$$

where Γ_i is a product of γ matrices, and F_i an invariant function. The second term in Eq. (2.14) is then

$$\sum_{\text{spin}} \text{Tr} \gamma_5 \mathbf{s} T_2^\dagger T_1 = \sum_i \text{Tr} \gamma_5 \mathbf{s} \Gamma_i^\dagger F_i^*. \quad (2.16)$$

Because of parity conservation, γ_5 in Γ_i should always occur in pairs and hence they can be eliminated by commuting through other γ matrices. We can write, therefore, $\Gamma_i = \mathbf{a}_1 \mathbf{a}_2 \cdots \mathbf{a}_{2n+1}$, where $n \geq 1$ and $\mathbf{a}_1 = a_{10} \gamma_0 - a_{1i} \gamma_i$. Because of Eq. (2.2), s has only the y components; hence,

$$\text{Tr} \gamma_5 \mathbf{s} \Gamma_i^\dagger = \text{Tr} \gamma_5 \mathbf{s} \gamma_0 (\mathbf{a}_{2n+1}^\dagger \cdots \mathbf{a}_2^\dagger \mathbf{a}_1^\dagger) \gamma_0.$$

Using the identities $\gamma_0^2 = 1$, $\gamma_0^\dagger = \gamma_0$, $\gamma_i^\dagger = -\gamma_i$, and $\gamma_0 \gamma_\mu^\dagger \gamma_0 = \gamma_\mu$, we obtain

$$\gamma_0 (\mathbf{a}_{2n+1}^\dagger \cdots \mathbf{a}_2^\dagger \mathbf{a}_1^\dagger) \gamma_0 = \mathbf{a}_{2n+1} \cdots \mathbf{a}_2 \mathbf{a}_1.$$

Hence,

$$\text{Tr} \gamma_5 \mathbf{s} \Gamma_i^\dagger = -\text{Tr} \mathbf{a}_{2n+1} \cdots \mathbf{a}_2 \mathbf{a}_1 \mathbf{s} \gamma_5 = -\text{Tr} \gamma_5 \mathbf{s} \Gamma_i. \quad (2.17)$$

From Eqs. (2.14)–(2.17), we obtain

$$A = \sum_i \text{Tr} \gamma_5 \mathbf{s} \Gamma_i 2i \text{Im} F_i. \quad (2.18)$$

This proves our assertion. It should be noted that $\text{Tr} \gamma_5 \mathbf{s} \Gamma_i$ is pure imaginary and hence A is real as it should be. When Feynman diagrams are used for the calculation, T invariance usually imposes a reality condition on the coupling constants, and unitarity implies that F_i in Eq. (2.18) can have an imaginary part only when it is kinematically possible for the intermediate states to be physical. Using this fact we can immediately conclude that diagrams shown in Figs. 4(a), 4(b), and 4(c) do not contribute to the up-down asymmetry; hence the diagrams shown in Fig. 2 contain all the diagrams needed to be considered for the up-down asymmetry. We notice that in both Figs. 2(a) and 2(b), the phases of the final states always get canceled out; hence the diagram in the left-hand side of Figs. 2(a) and 2(b) can be chosen to be real. If we choose this phase convention, the imaginary part of the matrix element in Fig. 2(a) can be obtained by replacing the Breit-Wigner formula for the resonant intermediate state f with its imaginary part

$$\text{Im} \frac{1}{(\Delta + p_2)^2 - M_R^2 + i\Gamma M_R} = \frac{-\Gamma M_R}{[(\Delta + p_2)^2 - M_R^2]^2 + \Gamma^2 M_R^2},$$

where M_R is the mass of the resonance and Γ is the width of the resonance with a proper threshold behavior. The imaginary part of the two-photon-exchange diagram,

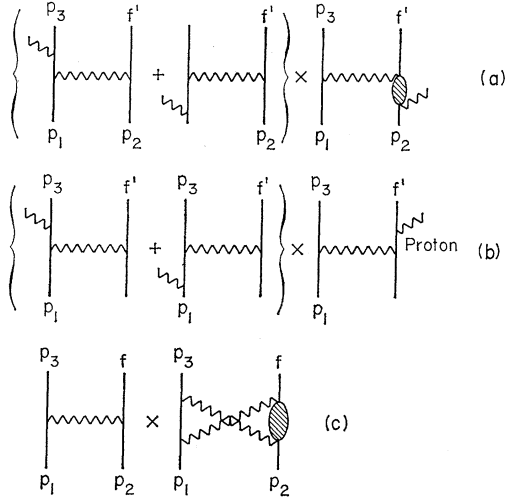


FIG. 4. Diagrams which change sign when e^- is replaced by e^+ but do not contribute to the asymmetry because no intermediate states are kinematically possible to be on the mass shell.

Fig. 2(b), can be obtained from the Cutkosky rule (see Appendix B). Indeed, if we let T_1 represent the matrix element of the Born term and T_2 represent the two-photon-exchange diagram, then Eq. (2.18) is equivalent to the statement that

$$A = \text{Tr} \gamma_5 S T_1^\dagger T_2 \text{out}, \quad (2.19)$$

where $T_2 \text{out}$ is obtained from T_2 by replacing the denominator of each of the propagators in the intermediate states by the following rule:

$$(p_i^2 - m_i^2)^{-1} \rightarrow 2\pi i \delta_+(p_i^2 - m_i^2).$$

When a set of Feynman diagrams is given, usually there is no ambiguity whatsoever as to how the asymmetry should be computed. The procedure sketched above is exactly what happens in the actual calculation. However, the reasoning given is not very rigorous. In Appendix A we give a more satisfactory derivation of the results of this section using T and P invariances and unitarity.

D. Both the real and imaginary parts⁸ of the two-photon-exchange diagram shown in Fig. 2(b) have infrared divergences when the hadron intermediate state is either a proton or equal to the final state f . However, it is well known that the infrared-divergent part of the matrix element is proportional to a product

⁸ Since we are always dealing with the interference between two matrix elements as given by Eq. (2.14), we need to know only the relative phase between T_1 and T_2 . However, it is convenient to define the phase of a matrix element so that the absorptive part of a matrix element corresponds to the imaginary part. This is automatically accomplished if we use the T -matrix elements instead of the S -matrix elements. In the text books, usually the Feynman rules for constructing the S -matrix elements are given. In order to obtain T -matrix elements, all one needs to do is to multiply the S -matrix element by a factor $-i$ (see Appendix B).

of the lowest-order Born diagram and a scalar function containing an infrared divergence factor.⁴ Since the lowest-order diagram does not produce an up-down asymmetry, we conclude that the infrared part of the two-photon-exchange diagram does not contribute to the up-down asymmetry. A simple demonstration of this fact is given in Appendix C.

E. It is well known that the real part of the two-photon-exchange diagram shown in Fig. 2(b) is not by itself gauge invariant; one has to add the criss-cross two-photon-exchange diagram Fig. 4(c) in order to have gauge invariance. However, the imaginary part of the two-photon-exchange diagram, Fig. 2(b), is gauge invariant. This can be seen easily if we remember that the imaginary part of this matrix element is obtained by putting both the electron and the hadron intermediate state on the mass shell. Since both the top and bottom part of the diagram are gauge invariant if the intermediate state is on the mass shell, their product must also be gauge invariant.

F. Since we are dealing with a very-high-energy electron, the mass of the electron can be ignored. In Appendix D, we show that because of gauge invariance, no singularity is induced by ignoring the mass of the electron when integrating with respect to the intermediate states in the two-photon-exchange diagram.

G. For completeness, let us reexpress the Christ-Lee theorem¹ in the case where the electromagnetic current operator j_μ has a component which does not transform according to Eq. (2.10). Let us decompose the current j_μ into two parts (normal and abnormal) $j_\mu = j_\mu^n + j_\mu^a$, where j_μ^n and j_μ^a behave differently under $X = PT$:

$$X j_i^n X^{-1} = j_i^n \quad \text{and} \quad X j_i^a X^{-1} = -j_i^a.$$

Equation (2.7) becomes then

$$B_{ij}^* = \sum_f [\langle p_2 \downarrow | j_i^n - j_i^a | f \rangle \langle f | j_j^n - j_j^a | p_2 \downarrow \rangle - \langle p_2 \uparrow | j_i^n - j_i^a | f \rangle \langle f | j_j^n - j_j^a | p_2 \uparrow \rangle] \times \delta^4(q + p_2 - p_f). \quad (2.20)$$

On the other hand, Eq. (2.6) gives

$$B_{ji}^* = B_{ij} = \sum_f [\langle p_2 \uparrow | j_i^n + j_i^a | f \rangle \langle f | j_j^n + j_j^a | p_2 \uparrow \rangle - \langle p_2 \downarrow | j_i^n + j_i^a | f \rangle \langle f | j_j^n + j_j^a | p_2 \downarrow \rangle] \times \delta^4(q + p_2 - p_f). \quad (2.21)$$

In Sec. II B, we have shown that when $j_i = j_i^n$, there is no asymmetry. It is also obvious from the derivation there that if $j_i = j_i^a$, there is also no asymmetry. Hence only the interference terms between j_i^n and j_j^a produce asymmetry. Since L^{ij} is symmetric, only the symmetric part of B_{ij} contributes to the cross section. Equation (2.6) says that the symmetric part of B_{ij} is its real part. Summing Eqs. (2.20) and (2.21), dividing the result by

2, and taking the real part, we obtain

$$\begin{aligned}
(B_{ij})^{\text{sym}} &\equiv \frac{1}{2}(B_{ij} + B_{ji}) \\
&= \text{Re} \sum_f [\langle p_2 \uparrow | j_i^n | f \rangle \langle f | j_j^a | p_2 \uparrow \rangle \\
&\quad + \langle p_2 \uparrow | j_i^a | f \rangle \langle f | j_j^n | p_2 \uparrow \rangle \\
&\quad - \langle p_2 \downarrow | j_i^n | f \rangle \langle f | j_j^a | p_2 \downarrow \rangle \\
&\quad - \langle p_2 \downarrow | j_i^a | f \rangle \langle f | j_j^n | p_2 \downarrow \rangle] \\
&\quad \times \delta^4(q + p_2 - p_f). \quad (2.22)
\end{aligned}$$

Applying the symmetry under a rotation operator $R = e^{i\pi J_z}$ to the first two terms in Eq. (2.22), and remembering that $|p_2 \uparrow\rangle$ is quantized along the y axis [$R|p_2 \uparrow\rangle = \eta_+ |p_2 \downarrow\rangle$, $R|p_2 \downarrow\rangle = \eta_- |p_2 \uparrow\rangle$], we obtain immediately

$$B_{xx}^{\text{sym}} = B_{yy}^{\text{sym}} = B_{zz}^{\text{sym}} = B_{xy}^{\text{sym}} = 0.$$

Hence only B_{xz}^{sym} and B_{yz}^{sym} are nonzero.

When no photons are emitted by the electrons, we have

$$L^{\mu\nu} = \frac{1}{2} \text{Tr}(\not{p}_1 + m)\gamma^\mu(\not{p}_3 + m)\gamma^\nu = 2(p_1^\mu p_3^\nu + p_1^\nu p_3^\mu + \frac{1}{2}q^2 g^{\mu\nu}). \quad (2.23)$$

Hence $L^{yz} = 0$, and

$$L^{xz} = [2(E_1^2 - E_3^2)/Q^2] |\mathbf{p}_1 \times \mathbf{p}_3|,$$

where all quantities are in the laboratory system and $Q^2 = (\mathbf{p}_1 - \mathbf{p}_3)^2$.

Since $L^{yz} = 0$, the asymmetry is proportional to

$$\begin{aligned}
N &= L^{xz}(B_{xz} + B_{zx}) + L^{x0}(B_{x0} + B_{0x}) \\
&= L_{xz}(B_{xz} + B_{zx})q^2/q_0^2 \\
&= \frac{4(E_1^2 - E_3^2)q^2}{q_0^2 Q^2} |\mathbf{p}_1 \times \mathbf{p}_3| \\
&\quad \times \text{Re} \int \frac{e^{-iq \cdot x}}{(2\pi)^4} d^4x \sum_{\text{spin of } p_2} \langle p_2 | \gamma_5 \mathcal{S} \\
&\quad \times [j_x^n(0)j_z^a(x) + j_x^a(0)j_z^n(x)] | p_2 \rangle. \quad (2.24)
\end{aligned}$$

Using the same normalization for j_μ and $|p_2\rangle$, the unpolarized cross section $d\sigma(\uparrow) + d\sigma(\downarrow)$ is proportional to $D = L^{\mu\nu} A_{\mu\nu}$, where

$$\begin{aligned}
A_{\mu\nu} &= \int \frac{e^{-iq \cdot x}}{(2\pi)^4} d^4x \\
&\quad \times \sum_{\text{spin of } p_2} \langle p_2 | j_\mu^n(0)j_\nu^n(x) + j_\mu^a(0)j_\nu^a(x) | p_2 \rangle \\
&= M^{-2} [\not{p}_2 \mu - q_\mu (\not{p}_2 \cdot q) / q^2] [\not{p}_2 \nu - q_\nu (\not{p}_2 \cdot q) / q^2] (-q^2 Q^{-2}) \\
&\quad \times (A_{xx} - q^2 q_0^{-2} A_{zz}) - (g_{\mu\nu} - q_\mu q_\nu / q^2) A_{xx}. \quad (2.25)
\end{aligned}$$

The asymmetry $A(T \text{ violation})$ defined in Eq. (1.1) is

then equal to

$$A(T \text{ violation}) = N/D. \quad (2.26)$$

Contracting the tensor in Eq. (2.25), we obtain

$$\begin{aligned}
D &= 2(E_1 E_3 + p_1 p_3 \cos \theta_{13} + m^2) (-q^2 Q^{-2}) (A_{xx} - q^2 q_0^{-2} A_{zz}) \\
&\quad + 4(E_1 E_3 - p_1 p_3 \cos \theta_{13} - 2m^2) A_{xx}.
\end{aligned}$$

Now Eq. (2.26) can be shown to be completely equivalent to Eq. (40) of Christ and Lee.¹ However, writing the asymmetry in the form of Eq. (2.24) has certain advantages: (a) It is more covariant looking, hence easier to apply when one is using Feynman diagrams. (b) It shows explicitly that the asymmetry is due to the interference between the matrix elements of j_x^n and j_z^a and between those of j_z^a and j_x^n . (c) It can be more easily compared to the formal expressions of Sec. V which relate to the asymmetry in the absence of T violation (see Sec. V).

III. BREMSSTRAHLUNG DIAGRAMS

In this section we show that the class of diagrams represented by Fig. 2(a) contributes negligibly to the up-down asymmetry. To show this we first argue that among all the diagrams which can be represented by Fig. 2(a), only the mechanism represented by Fig. 5 can possibly have a large contribution to the up-down asymmetry in the kinematical region we are interested in. We then show by an explicit calculation that Fig. 5 contributes negligibly to the up-down asymmetry compared with the experiment.

We are interested only in the kinematical region where f' in Fig. 2(a) is a proton or $N + \pi$, but the only hadron intermediate state f which can have any significant imaginary part in this kinematical region is $N^*(1238)$. When the final state f' is $N + \pi$, the photon emitted is necessarily soft. The matrix element for emission of a soft photon is proportional to the matrix element for no-photon emission and hence does not produce any up-down asymmetry. Therefore the final state f must be a proton. This shows that only the mechanism shown in Fig. 5 can possibly have any significant contribution to the up-down asymmetry in the kinematical region of interest.

In the following we proceed to calculate the up-down asymmetry due to the mechanism shown in Fig. 5. We

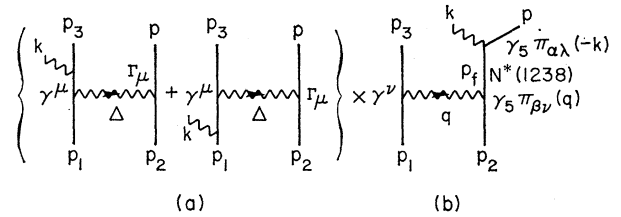


FIG. 5. Bremsstrahlung diagram which is likely to contribute to the up-down asymmetry when the missing mass is between one-pion and two-pion thresholds. p represents the final proton.

notice that this cross section can be calculated exactly in terms of the known experimental form factor for the $\gamma p N^*$ vertex. However, we have made an order-of-magnitude estimate of this cross section by making several reasonable approximations. We present this rough estimate of the cross section because the result happens to be too small to account for the observed asymmetry. We shall assume a pure $M1$ transition for the $\gamma p N^*$ vertex which can be written as⁹

$$e\bar{\Psi}_\beta(p_f)C_3(q^2)\gamma_5\pi_{\mu\beta}(q)u(p_2) = e\bar{\Psi}_\beta(p_f)C_3(q^2)\gamma_5 \times \left(\mathbf{q}g_{\beta\mu} - q_\beta\gamma_\mu + \frac{q \cdot p_f g_{\beta\mu}}{M_f} - \frac{q_\beta p_{f\mu}}{M_f} \right) u(p_2), \quad (3.1)$$

where $\Psi_\beta(p_f)$ is the Rarita-Schwinger spin- $\frac{3}{2}$ wave function, q is the momentum of the photon, $q + p_2 = p_f$, and $u(p_2)$ is the spinor representing the initial proton. C_3 is the form factor for the transition and can be written as⁹

$$C_3 M_p = 2.05 e^{-3.15\sqrt{(-q^2)}} [1 + 9\sqrt{(-q^2)}]^{1/2}. \quad (3.2)$$

The covariant spin sum for the spin- $\frac{3}{2}$ wave function is given by

$$\sum_{\text{spin}} \Psi_\alpha(p_f)\bar{\Psi}_\beta(p_f) \equiv G_{\alpha\beta} = (\mathbf{p}_f + M_f) \left[g_{\alpha\beta} - \frac{2}{3} p_{f\alpha} p_{f\beta} M_f^{-2} - \frac{1}{3} M_f^{-1} (p_{f\alpha} \gamma_\beta - p_{f\beta} \gamma_\alpha) - \frac{1}{3} \gamma_\alpha \gamma_\beta \right]. \quad (3.3)$$

In the rest frame of the 3-3 resonance, $p_f = (M_f, 0)$, $G_{00} = G_{\alpha 0} = 0$, and the space components of $G_{\alpha\beta}$ assume a very simple form

$$G_{ij} = \begin{bmatrix} \frac{1}{3} \sigma_i \sigma_j - \delta_{ij} & 0 \\ 0 & 0 \end{bmatrix} (2M_f). \quad (3.4)$$

$$\begin{aligned} d\sigma(\uparrow) - d\sigma(\downarrow) &= -e^6 \frac{1}{(2\pi)^5} 2i \left[\text{Im} \frac{1}{(q+p_2)^2 - M_{33}^2 + i\Gamma M_{33}} \right] \frac{1}{4M p_{11}} \int \frac{d^3 p_3}{2E_3} \frac{d^3 k}{2k} \frac{d^3 p}{2E} \delta^4(p_1 + p_2 - k - p - p_3)^{\frac{1}{2}} \\ &\times \text{Tr}(\mathbf{p}_1 + m) \gamma^\mu (\mathbf{p}_3 + m) \gamma^\nu \sum_{\text{photon pol}} \text{Tr} \gamma_5 \mathbf{s}(\mathbf{p}_2 + M) \Gamma_\mu(\mathbf{p} + M) e^\lambda (k g_{\alpha\lambda} - k_\alpha \gamma_\lambda + k \cdot p_f g_{\alpha\lambda} M_f^{-1} - k_\alpha p_{f\lambda} M_f^{-1}) \gamma_5 G^{\alpha\beta} \gamma_5 \\ &\times (\mathbf{q}g_{\beta\nu} - q_\beta \gamma_\nu + q \cdot p_f g_{\beta\nu} M_f^{-1} - q_\beta p_{f\nu} M_f^{-1}) \left(\frac{p_3 \cdot \epsilon}{p_3 \cdot k} - \frac{p_1 \cdot \epsilon}{p_1 \cdot k} \right) \frac{1}{q^4} C_3(0) C_3(q^2). \quad (3.8) \end{aligned}$$

The trace involving the electron line is

$$L^{\mu\nu} \equiv \frac{1}{4} \text{Tr}(\mathbf{p}_1 + m) \gamma^\mu (\mathbf{p}_3 + m) \gamma^\nu = p_1^\mu p_3^\nu + p_1^\nu p_3^\mu + (m^2 - p_1 \cdot p_3) g^{\mu\nu}. \quad (3.9)$$

The trace involving the baryon line is too complicated to be evaluated using the standard covariant techniques. We found that the easiest way to evaluate it is to go to the rest frame of N^* with coordinate axes defined by Fig. 3, to write all γ matrices in terms of σ matrices, and actually to multiply out the matrices. We use the

⁹ A. J. Dufner and Y. S. Tsai, Phys. Rev. 168, 1801 (1968).

Also, in the rest frame of the 3-3 resonance (R frame) the energy of the photon emitted is independent of the angle as long as the missing mass $(p_1 - p_3 + p_2)^2 = (k + p)^2$ is fixed. For these two reasons, we shall use the rest frame of the 3-3 resonance in our calculation.

The $\gamma p p$ vertex in Fig. 5(a) can be written as¹⁰

$$e\bar{u}(p) [a(t)\gamma_\mu - b(t)(p + p_2)_\mu] u(p_2) \equiv e\bar{u}(p) \Gamma_\mu(t) u(p_2), \quad (3.5)$$

where

$$a(t) \equiv G_m(t) = \frac{2.79}{(1-t/0.71)^2} = 2.79 G_e(t),$$

$$b(t) = \frac{G_m(t) - G_e(t)}{(1-t/4M^2) \times 2M},$$

and

$$t = (p - p_2)^2.$$

The matrix element for Fig. 5(a) is

$$\bar{u}(p_3) \left[\gamma \cdot \epsilon \frac{1}{\mathbf{p}_3 + \mathbf{k} - m} \gamma_\mu + \gamma_\mu \frac{1}{\mathbf{p}_1 - \mathbf{k} - m} \gamma \cdot \epsilon \right] u(p_1) \frac{1}{t} \bar{u}(p) \times \Gamma_\mu(t) u(p_2). \quad (3.6)$$

Since k is small compared with p_1 and p_3 , we approximate Eq. (3.6) by

$$\bar{u}(p_3) \gamma_\mu u(p_1) \frac{1}{q^2} \bar{u}(p) \Gamma_\mu(q^2) u(p_2) \left[\frac{p_3 \cdot \epsilon}{p_3 \cdot k} - \frac{p_1 \cdot \epsilon}{p_1 \cdot k} \right], \quad (3.7)$$

where

$$q^2 = (p_1 - p_3)^2.$$

With this approximation, the asymmetry can be written as (for $e^- + p$)

representation

$$\gamma_0 = \begin{bmatrix} 1 & 0 \\ 0 & -1 \end{bmatrix}, \quad \gamma_i = \begin{bmatrix} 0 & \sigma_i \\ -\sigma_i & 0 \end{bmatrix}, \quad \gamma_5 = \begin{bmatrix} 0 & 1 \\ 1 & 0 \end{bmatrix}, \quad (3.10)$$

and the radiation gauge for the photon.

We reduce the most complicated-looking part of the

¹⁰ Since we are going to evaluate the traces by explicitly multiplying γ matrices, it is convenient to choose an expression which contains the least number of γ matrices. Equation (3.5) for the $\gamma p p$ vertex was chosen for this reason.

matrix in the baryon trace into a simple form

$$\epsilon^\lambda \pi_{\lambda\alpha}(k) \gamma_5 G^{\alpha\beta} \gamma_5 \pi_{\nu\beta}(q) = \begin{bmatrix} C_\nu & 0 \\ 0 & 0 \end{bmatrix}, \quad (3.11)$$

where

$$\begin{aligned} C_0 &= C_z = 0, \\ C_x &= -\frac{2}{3} M_f Q [2(\mathbf{\epsilon} \times \mathbf{k})_y - i\{\epsilon_y(\boldsymbol{\sigma} \cdot \mathbf{k}) - k_y(\boldsymbol{\sigma} \cdot \boldsymbol{\epsilon})\}], \\ C_y &= \frac{2}{3} M_f Q [2(\mathbf{\epsilon} \times \mathbf{k})_x - i\{\epsilon_x(\boldsymbol{\sigma} \cdot \mathbf{k}) - k_x(\boldsymbol{\sigma} \cdot \boldsymbol{\epsilon})\}], \end{aligned}$$

and Q is the space component of q .

C_0 and C_z are zero because we have assumed that the transition $\gamma + p \rightarrow N^*$ is caused purely by a transverse photon. The C 's can also be written in a vector form

$$\mathbf{C} = \frac{2}{3} M_f \mathbf{Q} \times [(2 - i\boldsymbol{\sigma}) \times (\boldsymbol{\epsilon} \times \mathbf{k})]. \quad (3.12)$$

We see that \mathbf{C} is proportional to $(\boldsymbol{\epsilon} \times \mathbf{k})$, which is a consequence of our assumption that the decay $N^* \rightarrow p + \gamma$ is a pure magnetic dipole transition.

After all the γ matrices are multiplied together and traces taken, we sum the photon polarizations and carry out the integration with respect to the solid angle of the photon. Everything is straightforward but tedious. It is interesting to note, however, that the mass of the electron can be set equal to zero without giving any trouble in our integrations, and all the integrations can be carried out analytically. In fact, ignoring the mass of the electron, all the integrations with respect to the solid angle of the photon can be reduced into the following four types¹¹:

$$\int_0^{2\pi} d\psi \int_0^\pi \sin\theta d\theta \frac{(\cos^2\theta, \sin^2\theta \sin^2\psi, \sin^2\theta \sin^2\psi \cos\psi, \sin\theta \cos^2\theta \cos\psi)}{E_1 - p_1 \sin\theta \cos\psi} = (2\pi/p_1)(1, 1, \frac{1}{3}, \frac{1}{3}), \quad (3.13)$$

where $E_1 = (p_1^2 + m^2)^{1/2} \sim p_1$ is the energy of the incident electron.

After all the reductions and integrations, Eq. (3.8) can be written as

$$\frac{d\sigma}{d\Omega_3 dE_3}(\uparrow) - \frac{d\sigma}{d\Omega_3 dE_3}(\downarrow) = + \frac{2\alpha^3 p_{3l}}{3\pi M p_{1l}} \frac{\Gamma M_{33}}{(M_f^2 - M_{33}^2)^2 + \Gamma^2 M_{33}^2} \frac{1}{q^4} C_3(0) C_3(q^2) \chi_b, \quad (3.14)$$

where

$$\begin{aligned} \chi_b &= [k_R^2 (p_{1R} - p_{3R}) \sin\theta_{13R}] \left\{ a(q^2) (E_{2R} + M) \left(2 \frac{p_{1R}^2 p_{3R}^2}{Q^2} \sin^2\theta_{13R} - \frac{3}{2} q^2 + \frac{(p_{1R} + p_{3R})^2}{Q^2} p_{1R} p_{3R} \frac{q^2}{q_0^2} (1 - \cos\theta_{13R}) \right) \right. \\ &\quad + b(q^2) \left[-\frac{q^2}{2} (E_{2R} + M)(E_R + M) + \frac{k_R}{p_{1R} - p_{3R}} [\cos\theta_{13R} (p_{1R}^2 + p_{3R}^2) - 2p_{1R} p_{3R}] \left(\frac{2p_{1R}^2 p_{3R}^2}{Q^2} \sin^2\theta_{13R} - q^2 \right) \right. \\ &\quad \left. \left. - \frac{(p_{1R} + p_{3R})^2 p_{1R} p_{3R} q^2}{Q^2 q_0^2} (1 - \cos\theta_{13R}) [Q^2 + k_R (p_{1R} - p_{3R}) (1 + \cos\theta_{13R})] \right] \right\}. \quad (3.15) \end{aligned}$$

Here the subscripts l and R denote the laboratory frame and the rest frame of the N^* , respectively. In order to compare with the experiment, we approximate the cross section from an unpolarized proton target by the $e + p \rightarrow e + N^*$ cross section using the parametrization given by Dufner and Tsai,⁹ namely,

$$\begin{aligned} \frac{d\sigma}{d\Omega_3 dE_3}(\uparrow) + \frac{d\sigma}{d\Omega_3 dE_3}(\downarrow) &= \frac{4\alpha^2 p_{3l}}{3\pi p_{1l}} \left(\frac{M}{M_f} \right) \frac{\Gamma M_{33}}{(M_f^2 - M_{33}^2)^2 + \Gamma^2 M_{33}^2} \frac{1}{(-q^2)} \\ &\quad \times C_3^2(q^2) (E_{2R} + M) [Q^2 + (E_{1l} + E_{3l})^2]. \quad (3.16) \end{aligned}$$

From Eqs. (3.14) and (3.16), we obtain

$$\begin{aligned} A_b &= \left[\frac{d\sigma(\uparrow)}{d\Omega_3 dE_3} - \frac{d\sigma(\downarrow)}{d\Omega_3 dE_3} \right] / \left[\frac{d\sigma(\uparrow)}{d\Omega_3 dE_3} + \frac{d\sigma(\downarrow)}{d\Omega_3 dE_3} \right] \\ &= \frac{\alpha}{-2q^2} \frac{M_f C_3(0)}{M^2 C_3(q^2)} \\ &\quad \times \frac{\chi_b}{(E_{2R} + M) [Q^2 + (E_{1l} + E_{3l})^2]}, \quad (3.17) \end{aligned}$$

¹¹ We notice that in Eq. (3.8) the trace involving the lepton line $L_{\nu\nu}$ is symmetric with respect to the interchange $p_1 \leftrightarrow p_3$ and thus we need to consider only the term $p_1 \cdot \epsilon / p_1 \cdot k$ in $(p_3 \cdot \epsilon / p_3 \cdot k - p_1 \cdot \epsilon / p_1 \cdot k)$. The contribution from the other term $p_3 \cdot \epsilon / p_3 \cdot k$ can be obtained by a simple substitution $p_1 \rightarrow p_3$ after the integration with respect to the solid angle of k . In order to reduce the integrations into the forms shown in Eq. (3.13) we have to rotate the coordinate system from Fig. 3 into a new one where the x' axis is along p_1 and the z' axis is along $p_1 \times p_3$. In this coordinate system, many terms drop out because they are odd in ϕ .

where $C_3(q^2)$ and χ_b are given by Eqs. (3.2) and (3.15), respectively. In terms of E_{1l} , E_{3l} , and θ_{13l} , all the quantities appearing in Eqs. (3.15) and (3.17) can be computed (mass of the electron ignored) as follows:

$$\begin{aligned} M &= 0.938 \text{ GeV}, \quad \alpha = 1/137, \\ q^2 &= -4E_{1l}E_{3l} \sin^2(\frac{1}{2}\theta_{13l}), \\ M_f^2 &= q^2 + 2M(E_{1l} - E_{3l}) + M^2, \\ Q_l^2 &= E_{1l}^2 + E_{3l}^2 - 2E_{1l}E_{3l} \cos\theta_{13l}, \\ p_{1l} &= E_{1l}, \quad p_{3l} = E_{3l}, \\ k_R &= (M_f^2 - M^2)/2M_f, \quad p_{1R} = (ME_{1l} + \frac{1}{2}q^2)/M_f, \\ p_{3R} &= (M^2 + 2E_{1l}M - M_f^2)/2M_f, \quad Q_R = MQ_l/M_f, \\ \sin\theta_{13R} &= M p_{1l} p_{3l} \sin\theta_{13l} / (M_f p_{1R} p_{3R}), \\ q_{0R} &= (M_f^2 - M^2 + q^2)/2M_f, \\ E_{2R} &= (M_f^2 + M^2 - q^2)/2M_f, \end{aligned}$$

and

$$E_R = (M_f^2 + M^2)/2M_f.$$

In order to make an order-of-magnitude estimate of A_b , we notice that various quantities appearing in Eqs. (3.15) and (3.17) can be classified according to their magnitudes:

$$\begin{aligned} E_{1l}, E_{3l}, p_{1R}, p_{3R} &\sim 15 \text{ GeV}, \\ M, M_f, E_{2R}, E_R &\sim 1 \text{ GeV}, \\ -q^2, Q_l^2, Q_R^2 &\sim 0.5 \text{ GeV}^2, \\ k_R &\sim 0.3 \text{ GeV}, \\ q_{0R} = p_{1R} - p_{3R} &\sim 0.06 \text{ GeV}. \end{aligned}$$

Hence we can write, approximately,

$$\begin{aligned} A_b &\approx -\alpha \sin\theta_{13R} \frac{k_R^2}{4M q_{0R}} \frac{a(q^2)C_3(0)}{C_3(q^2)} \\ &\quad \times \left(1 - \frac{b(q^2)Q_R^2}{a(q^2)2M}\right) \approx -\alpha \sin\theta_{13R}, \end{aligned}$$

and thus we have proved that the asymmetry due to the bremsstrahlung emission is completely negligible.

IV. TWO-PHOTON-EXCHANGE CONTRIBUTION

In this section we consider a class of diagrams represented by Fig. 2(b). We are interested only in the hadron final states consisting of one pion plus one nucleon. The intermediate states can be a proton, various N^* 's, and continuum states. The only intermediate state one knows how to handle reliably is a proton, so we treat this case. In the kinematical region of interest, the final state $N+\pi$ is dominated by the formation of $N^*(1238)$ and the nonresonant s -wave part. The N^* excitation is mainly via magnetic dipole transition; the other two

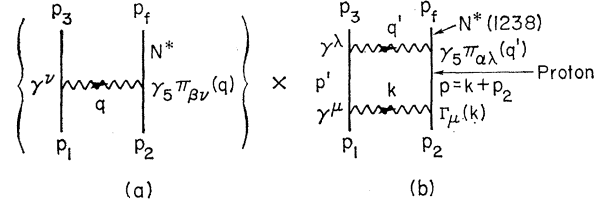


FIG. 6. Interference between one- and two-photon-exchange diagrams. The final hadron state is $N^*(1238)$ and the intermediate hadron state is a proton.

multipoles, $E2$ and $Q2$, contribute less than¹² 10% to the cross section. In this paper we ignore the nonresonant s -wave part as well as $E2$ and $Q2$ multipoles of the N^* excitation. The contribution to the asymmetry from the two-photon-exchange diagram with a proton as the intermediate state can be obtained from Eq. (2.19) with the help of the Cutkosky rule. The asymmetry can be written (for $e^- + p$) as

$$\begin{aligned} d\sigma(\uparrow) - d\sigma(\downarrow) &= -e^6 \frac{1}{(2\pi)^2} (-i) \frac{1}{4M p_{1ab}} \int \frac{d^3 p_3 d^3 p_f d^4 p'}{2E_3 2E_f (2\pi)^4} \\ &\quad \times \delta^4(p_1 + p_2 - p_3 - p_f) (2\pi i)^2 \delta_+(p'^2 - m^2) \\ &\quad \times \delta_+((p_1 + p_2 - p')^2 - M^2)^{\frac{1}{2}} \text{Tr}(\not{p}_1 + m) \gamma^\nu (\not{p}_3 + m) \\ &\quad \times \gamma^\lambda (\not{p}' + m) \gamma^\mu \text{Tr} \gamma_5 \not{s} (\not{p}_2 + M) \pi_{\nu\beta}(q) \gamma_5 G^{\beta\alpha} \gamma_5 \pi_{\lambda\alpha}(q') \\ &\quad \times (\not{p} + M) \Gamma_\mu(k) \frac{1}{q^2} \frac{1}{q'^2} \frac{1}{k^2} C_3(q^2) C_3(q'^2). \quad (4.1) \end{aligned}$$

The notations are given in Fig. 6. In order to simplify the calculation we shall ignore the spin of the electron.¹³ This approximation is equivalent to modifying the trace of the lepton current in Eq. (4.1) in the following way:

$$\begin{aligned} \frac{1}{2} \text{Tr}(\not{p}_1 + m) \gamma^\nu (\not{p}_3 + m) \gamma^\lambda (\not{p}_1 - k + m) \gamma^\mu \\ \times \frac{\longrightarrow}{\text{ignore electron spin}} (2p_1 - q)^\nu (2p_3 + q')^\lambda (2p_1 - k)^\mu \\ \equiv L^{\nu\lambda\mu}. \quad (4.2) \end{aligned}$$

Because of the current conservation q^ν , q'^λ , and k^μ can be dropped from $L^{\nu\lambda\mu}$; therefore we have

$$L^{\nu\lambda\mu} = 8p_1^\nu p_3^\lambda p_1^\mu. \quad (4.3)$$

The trace of the baryon current in Eq. (4.1) is almost identical to that of Eq. (3.8); hence we use the rest frame of the N^* with the coordinate axes defined by

¹² C. Mistretta, J. A. Appel, R. J. Budnitz, L. Carroll, J. Chen, J. R. Dunning, Jr., M. Goitein, K. Hanson, D. C. Imrie, and R. Wilson, Phys. Rev. **184**, 1487 (1969).

¹³ The severity of this approximation may be judged from its effect on the Born term. There we find that in Eq. (3.28) the factor $[Q_l^2 + (E_{1l} + E_{3l})^2]$ would be replaced by $[-Q_l^2 + (E_{1l} + E_{3l})^2]$ in the spinless-electron approximation. This is a very slight change in the kinematical region of interest.

Fig. 3 to calculate the trace,

$$\begin{aligned} B_{\mu\nu} &\equiv \text{Tr} \gamma_5 \mathbf{s}(\mathbf{p}_2 + M) \pi_{\nu\beta}(q) \gamma_5 G_{\beta\alpha} \gamma_5 \pi_{\lambda\alpha}(q') (\mathbf{p} + M) \Gamma_\mu(k) \\ &= -\text{Tr} \gamma_5 \mathbf{s}(\mathbf{p}_2 + M) \Gamma_\mu(k) (\mathbf{p} + M) \pi_{\lambda\alpha}(q') \\ &\quad \times \gamma_5 G_{\alpha\beta} \gamma_5 \pi_{\nu\beta}(q). \end{aligned} \quad (4.4)$$

The tensor $B_{\mu\nu}$ is nonzero only when ν is either x or y owing to Eqs. (3.11) and (3.12). The tensor $L^{\nu\lambda\mu}$ is zero when ν is y . Hence we need to consider only $\nu = x$ for $L^{\nu\lambda\mu} B_{\mu\nu}$. Similarly, $B_{\mu\nu}$ is nonzero only when λ is x , y , or z , but $L^{\nu\lambda\mu}$ is zero when $\lambda = y$; hence we need to consider only $\lambda = x$ and z for $L^{\nu\lambda\mu} B_{\mu\nu}$. We may write thus

$$\begin{aligned} L^{\nu\lambda\mu} B_{\mu\nu} &= -8 p_{1zR} \text{Tr} \gamma_5 \mathbf{s}(\mathbf{p}_2 + M) p_{1\mu} \Gamma_\mu(k) (\mathbf{p} + M) \\ &\quad \times \sum_{\lambda=x,z} p_{3\lambda} \pi_{\lambda\alpha}(q') \gamma_5 G^{\alpha\beta} \gamma_5 \pi_{\nu\beta}(q). \end{aligned} \quad (4.5)$$

From Eq. (3.12), we obtain

$$\sum_{\lambda=x,z} p_{3\lambda} \pi_{\lambda\alpha}(q') \gamma_5 G^{\alpha\beta} \gamma_5 \pi_{\nu\beta}(q) = \begin{bmatrix} C & 0 \\ 0 & 0 \end{bmatrix}, \quad (4.6)$$

where

$$C = -\frac{2}{3} M_f Q_R [2(\mathbf{p}_3 \times \mathbf{q}')_{yR} + i q'_{yR} (\mathbf{p}_3 \cdot \boldsymbol{\sigma})_R]. \quad (4.7)$$

The subscript R refers to the rest frame of the N^* and the coordinates are defined by Fig. 3. Substituting Eqs. (4.6) and (4.7) into Eq. (4.5), we obtain

$$L^{\nu\lambda\mu} B_{\mu\nu} = (16/3) i a Q_R p_{1zR} \chi, \quad (4.8)$$

where

$$\begin{aligned} \chi &= (E_{2R} + M) \{ 2[p_{1zR}(k_{zR} - Q_R) - k_{xR} p_{3zR}] \\ &\quad \times (k_{zR} p_{1zR} - k_{xR} p_{1zR}) + k_{yR}^2 (p_{1zR} Q_R - p_{1R}^2) \} \\ &\quad - Q_R \{ E_{1R} + [b(k^2)/a(k^2)] (2p_1 \cdot p_2 + k \cdot p_1) \} \\ &\quad \times \{ 2[p_{1zR}(k_{zR} - Q_R) - k_{xR} p_{3zR}] k_{xR} + k_{yR}^2 p_{3zR} \} \\ &\quad + 2Q_R k_{0R} p_{1zR} [p_{1zR}(k_{zR} - Q_R) - k_{xR} p_{3zR}]. \end{aligned} \quad (4.9)$$

In terms of χ , the asymmetry for $e^- + p$ scattering, Eq. (4.1), can be written as

$$\begin{aligned} \frac{d\sigma_{e^-}(\uparrow)}{dE_3 d\Omega_3} - \frac{d\sigma_{e^-}(\downarrow)}{dE_3 d\Omega_3} &= \frac{2\alpha^3 Q_R p_{1zR}}{3\pi M W p_{1C}} \\ &\quad \times \left(\frac{p_{3l}}{p_{1l}} \right) \frac{C_3(q^2)}{-q^2} \delta((p_2 + q)^2 - M_f^2) 2M_f I, \end{aligned} \quad (4.10)$$

where

$$I = \int_{\text{c.m.}} d\Omega_p \frac{p_{1C}^2}{k C^2 q'^2} \chi C_3(q^2) a(k^2). \quad (4.11)$$

The $d^4 p'$ integration in Eq. (4.1) was reduced into the form Eq. (4.1) with the help of two δ_+ functions in Eq. (4.1) in the c.m. system ($\mathbf{p}_1 + \mathbf{p}_2 = 0$). The cross section in Eq. (4.10) is the laboratory cross section.

χ as given in Eq. (4.9) is expressed in terms of the rest frame of N^* with the coordinate axes defined by Fig. 3, whereas $d\Omega_p$ integration is carried out in the c.m. system. The subscripts l , R , and C refer to the laboratory system, the rest frame of N^* , and the c.m.

system, respectively. When \mathbf{p}' is parallel to \mathbf{p}_1 , k_C is zero, and when \mathbf{p}' is parallel to \mathbf{p}_3 , the absolute value of q'^2 becomes minimum. When $(p_1 + p_2)^2 \equiv W^2 \gg M_f^2$, we have

$$q'^2_{\text{min}} \approx -(M_f^2 - M^2) 2m^2 / W^4, \quad (4.12)$$

which is zero if the mass of the electron is set equal to zero. These two singular points in the integrand of Eq. (4.11) are not true singularities: The integrand is finite at these two points *if we choose the variables of integrations properly*. To see this let us consider the case when \mathbf{p}' is almost parallel to \mathbf{p}_1 . k_C^2 is then proportional to θ^2 where θ is the angle between \mathbf{p}' and \mathbf{p}_1 . χ is proportional to k_C , hence it is proportional to θ , and the solid angle $d\Omega_p$ is $\sin\theta d\theta d\Omega$, which is linear in θ . Hence the integrand in Eq. (4.11) is finite when \mathbf{p}' is parallel to \mathbf{p}_1 *if the direction of \mathbf{p}' is chosen as the z axis*. This shows also that the asymmetry does not have the infrared divergence, as mentioned in the Introduction and Appendix C. Next we consider the case when \mathbf{p}' is almost parallel to \mathbf{p}_3 . If we ignore the mass of the electron, q'^2 is proportional to θ'^2 , where θ' is the angle between \mathbf{p}' and \mathbf{p}_3 . Because of the relation $\mathbf{p}' - \mathbf{p}_3 = \mathbf{q}'$, the quantity C in Eq. (4.7) is proportional to $\sin\theta'$ and hence χ is proportional to $\sin\theta'$. The solid angle is proportional to $\sin\theta'$ if the direction of \mathbf{p}_3 is chosen as the z axis. Hence the integrand in Eq. (4.11) is finite when \mathbf{p}' is parallel to \mathbf{p}_1 even if the mass of the electron is ignored, *provided that the direction of \mathbf{p}_3 is chosen as the z axis*. This shows also that the mass of the electron can be ignored in our problem, and that there is no $\ln m^2$ term in the asymmetry. In the numerical integration for Eq. (4.11), we divide the region of integration into two parts. In region I, we choose the direction of \mathbf{p}_1 as the z axis, then carry out the integration (4.11), setting the integrand to zero whenever the angle between \mathbf{p}' and \mathbf{p}_3 is smaller than $\frac{1}{2}\theta_{13C}$. In region II, we choose the direction of \mathbf{p}_3 as the z axis; then we integrate θ' from 0 to $\frac{1}{2}\theta_{13C}$. The sum of these two integrations gives I . We approximate again $d\sigma(\uparrow)/d\Omega_3 dE_3 + d\sigma(\downarrow)/d\Omega_3 dE_3$ by Eq. (3.16) and obtain

$$\begin{aligned} A_t &= \left(\frac{d\sigma(\uparrow)}{d\Omega_3 dE_3} - \frac{d\sigma(\downarrow)}{d\Omega_3 dE_3} \right)_{e^- + p} \bigg/ \left(\frac{d\sigma(\uparrow)}{d\Omega_3 dE_3} + \frac{d\sigma(\downarrow)}{d\Omega_3 dE_3} \right) \\ &= \frac{\alpha}{\pi W E_{1C} M^2 [Q_l^2 + (E_{1l} + E_{3l})^2] (E_{2R} + M) C_3(q^2)}, \end{aligned} \quad (4.13)$$

where I is given by Eq. (4.11).

In order to calculate A_t , we have to perform two Lorentz transformations ($R \rightarrow C \rightarrow L$) and two rotations [\mathbf{p}_3 as the z axis when \mathbf{p}' is almost parallel to \mathbf{p}_3 , otherwise \mathbf{p}_1 as the z axis; in Eq. (4.9) the z axis is along \mathbf{Q}], in addition to the twofold integrations with respect to the solid angle of \mathbf{p}' . We have done all these on a computer. Since it takes some effort to figure out the best way to handle all these calculations on a computer, we describe here how they can actually be done.

The following presentation also serves as a compact summary of the notation and kinematics. We first define the constants: $M=0.938$, $m=0.51\times 10^{-3}$, $\alpha=1/137$, and the laboratory quantities: E_{1l} (incident

electron energy in GeV), E_{3l} (outgoing electron energy in GeV), θ_l (electron scattering angle in radians). We then compute all quantities appearing in Eq. (4.13) in terms of E_{1l} , E_{3l} , and θ_l in the following sequence:

$$\begin{aligned} p_{1l} &= (E_{1l}^2 - m^2)^{1/2}, & p_{3l} &= (E_{3l}^2 - m^2)^{1/2}, & q^2 &= 2m^2 - 2(E_{1l}E_{3l} - p_{1l}p_{3l} \cos\theta_l), \\ \nu &= E_{1l} - E_{3l}, & Q_l^2 &= p_{1l}^2 + p_{3l}^2 - 2p_{1l}p_{3l} \cos\theta_l, & M_f^2 &= M^2 + 2M\nu + q^2, \\ M_f &= (M_f^2)^{1/2}, & W^2 &= m^2 + M^2 + 2E_{1l}M, & W &= (W^2)^{1/2}, & E_{1c} &= (m^2 + ME_{1l})/W, \\ E_{3c} &= (W^2 + m^2 - M_f^2)/2W, & p_{1c} &= (E_{1c}^2 - m^2)^{1/2}, & p_{3c} &= (E_{3c}^2 - m^2)^{1/2}, \\ \cos\theta_{13c} &= (q^2 - 2m^2 + 2E_{1c}E_{3c})/2p_{1c}p_{3c}, & \sin\theta_{13c} &= (1 - \cos^2\theta_{13c})^{1/2}, \\ E_{1R} &= [ME_{1l} + (\frac{1}{2}q^2)]/M_f, & E_{3R} &= (W^2 - m^2 - M_f^2)/2M_f, & E_{2R} &= (M\nu + M^2)/M_f, \\ Q_R &= MQ_l/M_f, & q_{0R} &= (q^2 + \nu M)/M_f, & p_{1zR} &= [E_{1R}q_{0R} - (\frac{1}{2}q^2)]/Q_R, \\ p_{1R} &= (E_{1R}^2 - m^2)^{1/2}, & p_{1xR} &= (p_{1R}^2 - p_{1zR}^2)^{1/2}, & p_{3zR} &= [E_{3R}q_{0R} + \frac{1}{2}q^2]/Q_R, \\ p_{3R} &= (E_{3R}^2 - m^2)^{1/2}, & p_{3xR} &= (p_{3R}^2 - p_{3zR}^2)^{1/2}, & \sin\theta_{13R} &= (p_{1c} \sin\theta_{13c})/p_{1R}. \end{aligned}$$

Integration in region I.

Variables of integration: θ and ϕ [see Fig. 7(a)].
Quantities containing variables of integration:

$$\begin{aligned} x &= \cos\theta \cos\theta_{13c} + \sin\theta \sin\theta_{13c} \cos\phi, \\ k_c^2 &= 2p_{1c}^2(1 - \cos\theta), & k_c &= (k_c^2)^{1/2}, \\ (\mathbf{k} \cdot \mathbf{p}_3)_c &= p_{1c}p_{3c}(\cos\theta_{13c} - x), & k_{0R} &= (\mathbf{k} \cdot \mathbf{p}_3)_c/M_f, \\ k_{zR} &= [k_{0R}q_{0R} + \frac{1}{2}k_c^2 - (\mathbf{k} \cdot \mathbf{p}_3)_c]/Q_R, \\ k_{yR} &= -p_{1c} \sin\theta \sin\phi, \\ k_{xR} &= \frac{1}{Q_R p_{1R} p_{3R} \sin\theta_{13R}} \{ [k_{0R}E_{3R} + (\mathbf{k} \cdot \mathbf{p}_3)_c] \\ &\quad \times (E_{1R}q_{0R} - \frac{1}{2}q^2) - (k_{0R}E_{1R} + \frac{1}{2}k_c^2) \\ &\quad \times (E_{3R}q_{0R} + \frac{1}{2}q^2) \}, \\ I_1 &= \int_{-1}^1 d\cos\theta \int_0^{2\pi} d\phi \frac{p_{1c}^2}{k_c^2 q'^2} \chi a(k^2) c_3(q'^2), \end{aligned}$$

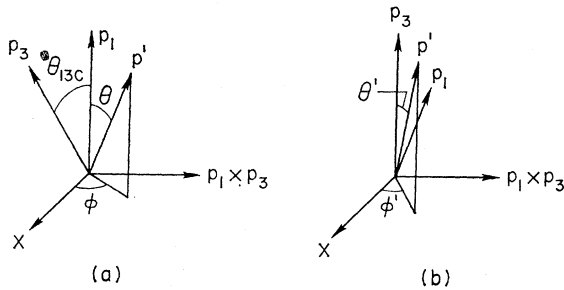


FIG. 7. Coordinate systems for the integration with respect to the solid angle of the intermediate electron p' in the two-photon-exchange diagram. When p' is almost parallel to p_1 , we choose p_1 as the z axis. When p' is almost parallel to p_3 , we choose p_3 as the z axis. These coordinate choices are essential in the numerical integrations in order to avoid the apparent singularities due to the two photon propagators.

where $x=0$ if $x > \cos\frac{1}{2}\theta_{13c}$; otherwise x is given by Eq. (4.9), $q'^2 = q^2 - 2(\mathbf{k} \cdot \mathbf{p}_3)_c$, $a(k^2) = 2.79(1 + k_c^2/0.71)^{-2}$, $b(k^2) = 1.79(2M)^{-1}(1 + k_c^2/4M^2)^{-1}(1 + k_c^2/0.71)^{-2}$, $c_3(q'^2) = M^{-1}2.05e^{-3.15(-q'^2)^{1/2}}[1 + 9(-q'^2)^{1/2}]^{1/2}$.

Integration in region II.

Variables of integration: θ' and ϕ' [see Fig. 7(b)].

$$\begin{aligned} I_2 &= \int_{\cos\frac{1}{2}\theta_{13c}}^1 d\cos\theta' \int_0^{2\pi} d\phi' \frac{p_{1c}^2}{k_c^2 q'^2} \chi a(k^2) c_3(q'^2), \\ k_c^2 &= 2p_{1c}^2(1 - \cos\theta_{13c} \cos\theta' + \sin\theta_{13c} \sin\theta' \cos\phi'), \\ k_c &= (k_c^2)^{1/2}, \\ (\mathbf{k} \cdot \mathbf{p}_3)_c &= p_{1c}p_{3c}(\cos\theta_{13c} - \cos\theta'), \\ k_{yR} &= -p_{1c} \sin\theta' \sin\phi'. \end{aligned}$$

All other expressions are identical to the integration in region I.

Compute $I = I_1 + I_2$ and then compute A_t using Eq. (4.13). The result is $A_t \approx 0.75 \times 10^{-2}$ for $e^- + p$ at $E_{1l} = 18$ GeV and $q^2 = -0.6$ GeV² for the missing mass ranging from the one- to the two-pion threshold. The reason why A_t is so insensitive to the missing mass is that the threshold behaviors of $\sigma(\uparrow) - \sigma(\downarrow)$ and $\sigma(\uparrow) + \sigma(\downarrow)$ cancel out upon taking the ratio in Eq. (4.3). Our value for A_t has the right sign compared with the experiment, but has the wrong shape and is one order of magnitude too small. Admittedly, we have made three drastic assumptions: (a) We kept only the proton intermediate state, (b) we ignored the s -wave background in the final state, and (c) our 3-3 resonance excitation contains only $M1$ and we ignored $Q2$ and $E2$ multipoles.

In order to see the effects of ignoring other intermediate states, we let the form factors appearing in the integration I in Eq. (4.3) be constant and we found that there is no significant change in the value of A_t thus obtained. This suggests (but does not prove) that including more intermediate states will not, in general,

make the asymmetry larger. In the radiative corrections to the e -unpolarized proton scattering, the correction is roughly $(2\alpha/\pi) \ln(-q^2/m^2) \ln(E/\Delta E)$. In the asymmetry there is no infrared divergence and also the mass of the electron can be ignored; hence terms such as $\ln E/\Delta E$ and $\ln(-q^2/m^2)$ cannot occur. Furthermore, besides α we have a small $\sin\theta_{13}$ to make the asymmetry small. Hence it is very difficult to make the asymmetry one order of magnitude larger than α at small scattering angles.

V. DISCUSSIONS

Bernstein, Feinberg, and Lee¹⁴ noticed that the ratio of amplitudes¹⁵ of $K_2 \rightarrow 2\pi$ to $K_1 \rightarrow 2\pi$ is roughly α/π and proposed the possibility that the CP noninvariance in the K_2 decay might be due to the electromagnetic interaction of hadrons. If we want to account for the apparent CP violation in the decay $K_2 \rightarrow 2\pi$ in terms of a possible CP violation in the electromagnetic interactions of hadrons, the abnormal current j_μ^a and the normal current j_μ^n of Eq. (2.24) must have strengths of the same order of magnitude. The experiment of Rock *et al.*³ shows that the asymmetry is less than 6%. This 6% asymmetry can be due to either a statistical fluctuation, an α^3 effect, or a genuine T violation. It is natural to ask whether one can obtain a lower limit for the ratio of the matrix element of j_i^a to that of j_i^n by assuming that this 6% asymmetry is all due to T violation. It should be noted that one cannot obtain an upper limit of $|\langle j_i^a \rangle / \langle j_i^n \rangle|$ from the asymmetry, because even if $|\langle j_i^a \rangle / \langle j_i^n \rangle|$ is large one can still get no asymmetry if the phases of the matrix elements conspire in a certain way. Ignoring the mass of the electron and using the properties of j_i^a and j_i^n under the operator $X=PT$, we can simplify Eq. (2.26) into

$$A(T \text{ violation}) = \frac{(E_1^2 - E_3^2) \cot^2 \frac{1}{2} \theta (-q^2/Q^2)(1/q_0^2)B}{2A_{xx} + \cot^2(\frac{1}{2}\theta) (-q^2/Q^2)[A_{xx} - (q^2/q_0^2)A_{zz}]}, \quad (5.1)$$

where

$$B = -4 \operatorname{Re} \sum_f [\langle p_2 \uparrow | j_z^n | f \rangle \langle f | j_z^a | p_2 \uparrow \rangle + \langle p_2 \uparrow | j_z^n | f \rangle \langle f | j_x^a | p_2 \uparrow \rangle] \delta^4(q + p_2 - p_f),$$

$$A_{xx} = 2 \sum_f [|\langle p_2 \uparrow | j_z^n | f \rangle|^2 + |\langle p_2 \uparrow | j_x^a | f \rangle|^2] \times \delta^4(q + p_2 - p_f)$$

$$\equiv 2[(J_z^n)^2 + (J_x^a)^2], \quad (5.2)$$

and

$$A_{zz} = 2 \sum_f [|\langle p_2 \uparrow | j_z^n | f \rangle|^2 + |\langle p_2 \uparrow | j_z^a | f \rangle|^2] \times \delta^4(q + p_2 - p_f)$$

$$\equiv 2[(J_z^n)^2 + (J_z^a)^2].$$

Here

$$J_z^n \equiv \left[\sum_f |\langle p_2 \uparrow | j_z^n | f \rangle|^2 \delta^4(q + p_2 - p_f) \right]^{1/2},$$

$$J_z^a \equiv \left[\sum_f |\langle p_2 \uparrow | j_z^a | f \rangle|^2 \delta^4(q + p_2 - p_f) \right]^{1/2},$$

$$J_x^a \equiv \left[\sum_f |\langle p_2 \uparrow | j_x^a | f \rangle|^2 \delta^4(q + p_2 - p_f) \right]^{1/2},$$

$$J_z^a \equiv \left[\sum_f |\langle p_2 \uparrow | j_z^a | f \rangle|^2 \delta^4(q + p_2 - p_f) \right]^{1/2}.$$

Using the inequalities $\mathbf{A} \cdot \mathbf{B} \leq |\mathbf{A}| |\mathbf{B}|$ and $|\mathbf{A} + \mathbf{B}| \leq |\mathbf{A}| + |\mathbf{B}|$, we obtain

$$|B| \leq 4(J_z^n J_z^a + J_x^a J_z^a),$$

$$\frac{|B|}{A_{xx}} \leq \frac{2J_z^n J_z^a}{(J_z^n)^2 + (J_z^a)^2} \left(\frac{J_z^a}{J_z^n} + \frac{J_x^a}{J_z^n} \right). \quad (5.3)$$

Hence

$$\frac{|B|}{A_{xx}} \leq \left[1 + \frac{Rq_0^2}{(-q^2)} \right] \left(\frac{J_z^a}{J_z^n} + \frac{J_x^a}{J_z^n} \right), \quad (5.4)$$

where¹⁶

$$R \equiv \frac{\sigma_l}{\sigma_T} \equiv \frac{(-q^2/q_0^2)A_{zz}}{A_{xx}}.$$

From Eqs. (5.1) and (5.4) we obtain

$$\left(\frac{J_z^a}{J_z^n} + \frac{J_x^a}{J_z^n} \right) \geq A(T \text{ violation})$$

$$\times \frac{2 + \cot^2(\frac{1}{2}\theta) (-q^2/Q^2)(1+R)}{(E_1 + E_3)q_0^{-1} \cot^2 \frac{1}{2} \theta (-q^2/Q^2) [1 + Rq_0^2/(-q^2)]}. \quad (5.5)$$

In the kinematic region of the bump in Fig. 1, we obtain

$$J_z^a/J_z^n + J_x^a/J_z^n \geq |A(T \text{ violation})| (1+R)/1.2.$$

Therefore the measurement of $A(T \text{ violation})$ of Eq. (1.1) gives a lower bound on $J_z^a/J_z^n + J_x^a/J_z^n$, and if $R = \sigma_l/\sigma_T$ is of order 1, then the magnitude of $A(T \text{ violation})$ is roughly equal to this lower bound. Since we cannot give an upper bound for J_z^a and J_x^a from a given $A(T \text{ violation})$ even if $A(T \text{ violation})$ is equal to zero, we cannot say that the T -violating current j_μ^a is equal to zero. However, it will take some miraculous cancellations among various terms in Eq. (5.2) to give zero asymmetry when j_i^a is comparable to j_i^n . This

¹⁴ J. Bernstein, G. Feinberg, and T. D. Lee, Phys. Rev. **139**, B1650 (1965).

¹⁵ J. H. Christenson, J. W. Cronin, V. I. Fitch, and R. Turlay, Phys. Rev. Letters **13**, 138 (1964).

¹⁶ L. H. Hand, Phys. Rev. **129**, 1834 (1963).

would be especially true if $A(T$ violation) is zero at all energies and angles. Hence the smallness of the asymmetry found by Rock *et al.*³ indicates that T is a good symmetry in the electromagnetic interaction of hadrons, and the apparent CP violation of $K_2 \rightarrow 2\pi$ decay is very unlikely to be due to the electromagnetic interactions.

The maximum allowed asymmetry for any given value of R can be obtained from the inequality (5.3) and

$$|B| \leq 4(J_x^n J_z^a + J_z^n J_x^a) \leq 2(A_{xx} A_{zz})^{1/2}. \quad (5.6)$$

The last inequality is equivalent to Eq. (27) of Christ and Lee. From (5.5) and (5.1) we obtain

$$|A(T \text{ violation})| \leq \frac{2(E_1 + E_3)(E_1 E_3 R)^{1/2} \cos^2 \frac{1}{2} \theta}{Q^2 + 2E_1 E_3 (1 + R) \cos^2(\frac{1}{2} \theta)}. \quad (5.7)$$

For small angles and small energy loss, the inequality (5.7) reduces to

$$|A(T \text{ violation})| \leq 2R^{1/2}/(1+R). \quad (5.8)$$

The right-hand side is maximum when $R=1$, and the maximum allowed $|A(T \text{ violation})|$ is equal to 1 when $R=1$.

Let us next discuss the asymmetry due to the α^3 cross sections. We have shown that the asymmetries due to both the bremsstrahlung and the two-photon exchange have neither the infrared divergence nor the divergence due to $m^2 \rightarrow 0$. For this reason it is very difficult to obtain an asymmetry which is one order of magnitude larger than α . The arguments given in Sec. III to show that A_b is small are convincing. For A_t , we do not know how to calculate the cross section if the intermediate state is not a proton. We can improve the treatment of final states in our calculation of A_t . We can include the small Q^2 and E^2 amplitudes for the N^* excitation by using more recent data.¹² The contribution from the nonresonant s -wave part can be estimated by first using the Nambu-Shrauner formula¹⁷ to evaluate the blobs in Figs. 8(a) and 8(b), and then calculating the contributions from these diagrams to the asymmetry. It should be noted however that adding more intermediate states or final states to the calculation does not necessarily increase the magnitude of the

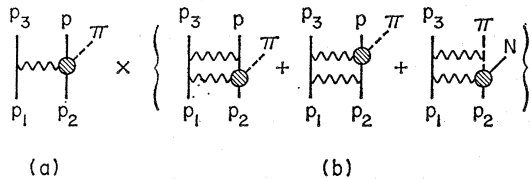


FIG. 8. Feynman diagrams for calculating the asymmetry due to the s -wave pion production. Blobs in these diagrams can be obtained from the Nambu-Shrauner formula.

¹² Y. Nambu and E. Shrauner, Phys. Rev. 128, 862 (1962); S. L. Adler and F. J. Gilman, *ibid.* 152, 1460 (1966); Y. Nambu and M. Yoshimura, Phys. Rev. Letters 24, 25 (1970).

asymmetry. In fact, it has been shown by Guerin and Piketty⁵ for the case of the elastic scattering that the various intermediate states give contributions of roughly the same order of magnitude and with more or less random signs. Hence, in order to estimate the order of magnitude of the asymmetry, any reasonable choice of intermediate states or final states will give a correct estimate.

The general expression for the asymmetry due to the two-photon exchange can be obtained from generalizing Eq. (4.1) to include all intermediate and final states [see Fig. 2(b) for notations]:

$$\begin{aligned} \frac{d\sigma(\uparrow)}{d\Omega_3 dE_3} - \frac{d\sigma(\downarrow)}{d\Omega_3 dE_3} &= \mp i \frac{e^6}{(2\pi)^3} \frac{p_{3t}}{8M p_{11}} \\ &\times \int \frac{d^3 p'}{2E'(2\pi)^3} \frac{1}{q'^2 k^2 q^2} \frac{1}{2} \text{Tr}(\mathbf{p}_1 + m) \gamma^\nu (\mathbf{p}_3 + m) \\ &\times \gamma^\lambda (\mathbf{p}' + m) \gamma^\mu \sum_{\text{spin of } p_2} \int e^{i\mathbf{q} \cdot \mathbf{x}} e^{-i\mathbf{k} \cdot \mathbf{y}} d^4 x d^4 y \\ &\times \langle p_2 | \gamma_5 \mathbf{s} j_\nu(x) j_\lambda(0) j_\mu(y) | p_2 \rangle, \end{aligned} \quad (5.9)$$

where $q = p_1 - p_3$, $k = p_1 - p'$, and $q' = p' - p_3$. The minus sign is for $e^- + p$ scattering. Using the same normalization, two times the cross section from an unpolarized proton target can be written as

$$\begin{aligned} \frac{d\sigma(\uparrow)}{d\Omega_3 dE_3} + \frac{d\sigma(\downarrow)}{d\Omega_3 dE_3} &= \frac{e^4}{(2\pi)^3} \frac{p_{3t}}{8M p_{11}} \frac{1}{q^4} \frac{1}{2} \text{Tr}(\mathbf{p}_1 + m) \\ &\times \gamma^\lambda (\mathbf{p}_3 + m) \gamma^\mu \sum_{\text{spin of } p_2} \int e^{-i\mathbf{q} \cdot \mathbf{y}} d^4 y \\ &\times \langle p_2 | j_\lambda(0) j_\mu(y) | p_2 \rangle. \end{aligned} \quad (5.10)$$

From Eq. (5.9) we can obtain the expression for the contribution from any final and intermediate states by simply inserting them between the currents $j_\nu(x)$, $j_\lambda(0)$, and $j_\mu(y)$. For example the up-down asymmetry in elastic ep scattering can be obtained from Eq. (5.9) by inserting the final proton state $\sum_{\text{spin of } p} |p\rangle \langle p| \times d^3 p (2E)^{-1} (2\pi)^{-3}$ between $j_\nu(x)$ and $j_\lambda(0)$ in Eq. (5.9). We obtain

$$\begin{aligned} \left(\frac{d\sigma(\uparrow)}{d\Omega_3} - \frac{d\sigma(\downarrow)}{d\Omega_3} \right)_{\text{elastic}} &= \mp i \frac{e^6}{(2\pi)^3} \frac{\pi}{8} \left(\frac{E_{11}}{M E_{31}} \right)^2 \\ &\times \int \frac{d^3 p'}{2E'(2\pi)^3} \frac{1}{q'^2 k^2 q^2} \frac{1}{2} \text{Tr}(\mathbf{p}_1 + m) \gamma^\nu (\mathbf{p}_3 + m) \\ &\times \gamma^\lambda (\mathbf{p}' + m) \gamma^\mu \sum_{\text{spin of } p_2 \text{ and } p} \int e^{-i\mathbf{k} \cdot \mathbf{y}} d^4 y \\ &\times \langle p_2 | \gamma_5 \mathbf{s} j_\nu(0) | p \rangle \langle p | j_\lambda(0) j_\mu(y) | p_2 \rangle. \end{aligned} \quad (5.11)$$

In general, even if we know the unpolarized cross section, Eq. (5.10), from experiment for all q^2 and q_0 , we still do not know how to calculate Eq. (5.9) or, for that matter, even Eq. (5.11). The reason is that in Eq. (5.11) both the spin and momentum of $|p\rangle$ can be different from those of $|p_2\rangle$.

The only thing common among Eqs. (5.9)–(5.11) is that they all involve products of currents at different points in space-time. Hence if one has some model for products of operators at different points in space-time, it can be tested against the experimental results using Eqs. (5.9)–(5.11). As far as we know, no one has ever proposed such a model.

For completeness of discussion let us consider the contribution of two-virtual-photon emission and absorption from a hadron current to other observable physical phenomena.

A. Radiative Correction to Electron Scattering from an Unpolarized Proton Target

In this case only the *real parts* of the two-photon-exchange diagrams, Fig. 4(c) and Fig. 2(b), contribute. The two diagrams must be considered together because of gauge invariance. Both diagrams have infrared divergences when the intermediate state is equal either to the initial or to the final state. The real part of the two-photon exchange is related to the imaginary part by dispersion relations. However, the imaginary part required here is not the part which appears in the up-down asymmetry, but the one obtainable from Eq. (5.9) without $\gamma_5 \mathbf{s}$. These two “imaginary parts” of the two-photon-exchange diagrams are completely independent of each other. This can be seen easily if we go to the laboratory frame where $|p_2\rangle$ becomes a two-component spinor and $\gamma_5 \mathbf{s}$ reduces to a 2×2 matrix $\mathbf{s} \cdot \boldsymbol{\sigma}$, and $j_\nu(x) j_\lambda(0) j_\mu(y)$ can also be reduced into a 2×2 matrix which can be represented in general by $A + \mathbf{B} \cdot \boldsymbol{\sigma}$. We have, then,

$$\sum_{\text{spin of } p_2} \langle p_2 | \gamma_5 \mathbf{s} j_\nu(x) j_\lambda(0) j_\mu(y) | p_2 \rangle \rightarrow \text{Tr}[\mathbf{s} \cdot \boldsymbol{\sigma}(A + \mathbf{B} \cdot \boldsymbol{\sigma})] = 2\mathbf{s} \cdot \mathbf{B},$$

whereas

$$\sum_{\text{spin of } p_2} \langle p_2 | j_\nu(x) j_\lambda(0) j_\mu(y) | p_2 \rangle = \text{Tr}(A + \mathbf{B} \cdot \boldsymbol{\sigma}) = 2A;$$

thus the two expressions are entirely independent of each other.

B. Hyperfine Shift of Hydrogen Atom

Iddings¹⁸ showed that the two-photon-exchange contribution to the hyperfine shift in the ground state of a hydrogen atom is related to the cross section of polarized electrons on polarized protons if there are no subtraction terms in the dispersion relations. From Eq. (3.4) of

Iddings's paper we see that the quantity needed is

$$\sum_{\text{spin of } p_2} \int e^{-i\mathbf{q} \cdot \mathbf{y}} d^4 y \langle p_2 | \gamma_5 \mathbf{s} j_\lambda(0) j_\mu(y) | p_2 \rangle, \quad (5.12)$$

which looks like the expression in Eq. (5.10) except for the operator $\gamma_5 \mathbf{s}$. Using the same argument as in Sec. V A, we see that the two expressions are independent of each other. Let us consider the relation between Eqs. (5.11) and (5.12). In Eq. (5.11), the factor $\langle p_2 | \gamma_5 \mathbf{s} j_\nu(0) | p \rangle$ is known for all combinations of spins of p_2 and p . The expectation value in Eq. (5.12) can be written as

$$\sum_{\text{spin of } p_2} \langle p_2 | \gamma_5 \mathbf{s} j_\lambda(0) j_\mu(y) | p_2 \rangle \equiv \langle p_2 \uparrow | j_\lambda(0) j_\mu(y) | p_2 \uparrow \rangle - \langle p_2 \downarrow | j_\lambda(0) j_\mu(y) | p_2 \downarrow \rangle,$$

whereas the last factor of Eq. (5.11) contains

$$\langle p \uparrow | j_\lambda(0) j_\mu(y) | p_2 \downarrow \rangle, \quad \langle p \uparrow | j_\lambda(0) j_\mu(y) | p_2 \uparrow \rangle, \quad \text{etc.},$$

where in general $p_2 \neq p$. Hence if one knows how to calculate Eq. (5.11) one can certainly calculate Eq. (5.12), but not the other way around.

ACKNOWLEDGMENTS

We would like to thank members of Berkeley-SLAC collaboration who did the experiment for showing us their experimental data in advance of publication and for useful conversations. One of us (R.N.C.) would also like to acknowledge a valuable conversation with C. Quigg.

APPENDIX A

In this appendix we give an alternative proof that the α^3 contribution to the up-down asymmetry is given completely by the imaginary part of the diagrams shown in Figs. 2(a) and 2(b). In Sec. II C we have shown this by using the properties of Feynman diagrams. In this appendix we show this directly using T and P invariances and the unitarity of the S matrix.

Let us write the S matrix in the form

$$\langle f | S | i \rangle = \delta_{if} + i(2\pi)^4 \delta^4(p_f - p_i) \langle f | A | i \rangle, \quad (A1)$$

where

$$A = (eA_1 + e^2A_2 + e^3A_3 + \dots). \quad (A2)$$

Unitarity of S gives

$$\begin{aligned} \langle f | A^\dagger | i \rangle &= \langle f | A | i \rangle - i(2\pi)^4 \\ &\times \sum_n \langle f | A | n \rangle \langle n | A^\dagger | i \rangle \delta^4(p_i - p_n). \end{aligned} \quad (A3)$$

The asymmetry is proportional to

$$\begin{aligned} \Delta &= \sum_{\lambda_f, \lambda_1, \lambda_3} \{ |\langle p_3 \lambda_3 p_f \lambda_f | A | p_1 \lambda_1 p_2 \uparrow \rangle|^2 \\ &\quad - |\langle p_3 \lambda_3 p_f \lambda_f | A | p_1 \lambda_1 p_2 \downarrow \rangle|^2 \}. \end{aligned} \quad (A4)$$

¹⁸ C. K. Iddings, Phys. Rev. **138**, B446 (1965).

We consider this in the laboratory system, Fig. 3. λ_1 , λ_3 , and λ_f are helicity states and $|\uparrow\rangle$ and $|\downarrow\rangle$ are eigenfunctions of angular momentum J_y for the initial proton. Decomposing $|\uparrow\rangle$ and $|\downarrow\rangle$ also into helicity states

$$|\uparrow\rangle = (1/\sqrt{2})(|\frac{1}{2}\rangle + i|\frac{-1}{2}\rangle)$$

and

$$|\downarrow\rangle = (1/\sqrt{2})(|\frac{1}{2}\rangle - i|\frac{-1}{2}\rangle),$$

we can write Eq. (A4) as

$$\Delta = -2 \operatorname{Im} \sum_{\lambda_1 \lambda_3 \lambda_f} \langle p_3 \lambda_3 p_f \lambda_f | A | p_1 \lambda_1 p_2 \frac{1}{2} \rangle^* \times \langle p_3 \lambda_3 p_f \lambda_f | A | p_1 \lambda_1 p_2 - \frac{1}{2} \rangle. \quad (\text{A5})$$

The time-reversal invariance implies

$$\langle f | A | i \rangle^* = \langle T f | A^\dagger | T i \rangle. \quad (\text{A6})$$

Let us use the coordinate system defined by Fig. 3 and let R be a rotation by π about the y axis. Then we have

$$RT | p_2 \lambda_2 \rangle = \eta | p_2 \lambda_2 \rangle, \quad (\text{A7})$$

where η is a phase independent of λ_2 .

Using Eqs. (A6) and (A7), Eq. (A5) can be written as

$$\Delta = -2 \operatorname{Im} \sum_{\lambda_1 \lambda_3 \lambda_f} \langle p_3 \lambda_3 p_f \lambda_f | A^\dagger | p_1 \lambda_1 p_2 \frac{1}{2} \rangle \times \langle p_3 \lambda_3 p_f \lambda_f | A^\dagger | p_1 \lambda_1 p_2 - \frac{1}{2} \rangle^*. \quad (\text{A8})$$

Substituting the unitarity relation (A3) into (A8), adding the resultant Δ to the Δ obtained in Eq. (A5), and dividing the expression by 2, we obtain

$$\Delta = -\operatorname{Im} \sum_{\lambda_1 \lambda_3 \lambda_f} \{ -i(2\pi)^4 [\langle |\delta^4 A A^\dagger | \frac{1}{2} \rangle \langle |A| - \frac{1}{2} \rangle^* - \langle |A | \frac{1}{2} \rangle \langle |\delta^4 A A^\dagger | - \frac{1}{2} \rangle^*] + (2\pi)^8 \langle |\delta A A^\dagger | \frac{1}{2} \rangle \times \langle |\delta^4 A A^\dagger | - \frac{1}{2} \rangle^* \}, \quad (\text{A9})$$

where we have used the short-hand notations

$$\langle | \equiv \langle p_3 \lambda_3 p_f \lambda_f |, \quad | \frac{1}{2} \rangle \equiv | p_1 \lambda_1 p_2 \frac{1}{2} \rangle,$$

and

$$| - \frac{1}{2} \rangle \equiv | p_1 \lambda_1 p_2 - \frac{1}{2} \rangle, \\ \delta^4 A A^\dagger \equiv \sum_n \delta^4(p_i - p_n) A | n \rangle \langle n | A^\dagger.$$

Applying the antiunitary operator RT defined in (A7), we see that the last term in Eq. (A9) is real and therefore can be ignored. The first two terms in Eq. (A9) can be further simplified by using the invariance under $Y = e^{-i\pi J_y} P$.

Since $Y | p \lambda \rangle = \eta' (-1)^{s-\lambda} | p - \lambda \rangle$, where η' is a phase independent of p and λ , we have $Y | \frac{1}{2} \rangle Y | - \frac{1}{2} \rangle^* = - | - \frac{1}{2} \rangle \times | \frac{1}{2} \rangle^*$. Thus Eq. (A9) can be written as

$$\Delta = 2 \operatorname{Re} \sum_{\lambda_1 \lambda_3 \lambda_f} (2\pi)^4 \langle |\delta^4 A A^\dagger | \frac{1}{2} \rangle \langle |A | - \frac{1}{2} \rangle^*. \quad (\text{A10})$$

For the α^3 contribution to Δ , A in $\langle |A | - \frac{1}{2} \rangle^*$ can be either $e^2 A_2$ or $e^3 A_3$. In the former case, $\langle |i\delta^4 A A^\dagger | \frac{1}{2} \rangle$

represents the absorptive part of the two-photon-exchange diagrams. In the latter case, $\langle |A | - \frac{1}{2} \rangle^*$ represents the bremsstrahlung emission from the electron lines and $\langle |\delta^4 A A^\dagger | \frac{1}{2} \rangle$ represents the absorptive part of the bremsstrahlung emission from the hadrons. In both of these cases $\langle |A | - \frac{1}{2} \rangle^*$ in Eq. (A10) does not have any absorptive part; hence, $A^\dagger = A$ for this matrix element. Changing from the helicity representation back into the angular momentum representation, we have

$$\Delta = \operatorname{Re} \sum_{\lambda_1 \lambda_3 \lambda_f} i(2\pi)^4 \{ \langle |\delta^4 A A^\dagger | \uparrow \rangle \langle |A | \uparrow \rangle^* - \langle |\delta^4 A A^\dagger | \downarrow \rangle \langle |A | \downarrow \rangle^* + \langle |\delta^4 A A^\dagger | \downarrow \rangle \langle |A | \uparrow \rangle^* - \langle |\delta^4 A A^\dagger | \uparrow \rangle \langle |A | \downarrow \rangle^* \}. \quad (\text{A11})$$

Applying the invariance under PT , Eqs. (2.8) and (2.9), to the first and third terms inside the parentheses and using $PTA(PT)^{-1} = A^\dagger$, we see that the first term is the complex conjugate of the second and the third term is (-1) times the complex conjugate of the fourth. Hence the third and fourth terms and the Re symbol can be dropped from Eq. (A11):

$$\Delta = e^6 \sum_{\lambda_1 \lambda_2 \lambda_3 \lambda_f} [\langle |A_2 \gamma_5 \mathbf{s} | \lambda_2 \rangle^* \langle |i(2\pi)^4 \delta^4 A_2 A_2^\dagger | \lambda_2 \rangle + \langle |A_3 \gamma_5 \mathbf{s} | \lambda_2 \rangle^* \langle |i(2\pi)^4 \delta^4 A_1 A_2^\dagger | \lambda_2 \rangle]. \quad (\text{A12})$$

The first term corresponds to the class of diagrams represented by Fig. 2(b) and the second term corresponds to those diagrams represented by Fig. 2(a). Hence we have reproduced all the results contained in Sec. II C without using the properties of γ matrices. From Eqs. (A2) and (A3) we see that $\langle |i(2\pi)^4 \delta^4 A_2 A_2^\dagger | \lambda_2 \rangle$ in Eq. (A12) is $2i$ times the imaginary part of the two-photon-exchange diagram $\langle |A_4 | \lambda_2 \rangle$, and hence can be obtained from Cutkosky rule Eq. (B5).

APPENDIX B

In Sec. IV we have used the Cutkosky rule¹⁹ to obtain the imaginary part of the two-photon-exchange diagram. It is easy to see that the rule, as applied in our calculation, is equivalent to the unitarity relation. Using the notation of Appendix A, the unitarity of the S matrix gives

$$\langle |A_4 - A_4^\dagger | \lambda_2 \rangle = \langle |i(2\pi)^4 \delta^4 A_2^\dagger A_2 | \lambda_2 \rangle. \quad (\text{B1})$$

Suppose we are interested in the contribution from an intermediate state consisting of one electron denoted

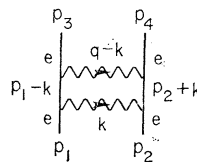


FIG. 9. Two-photon-exchange diagram for electron-electron scattering used to illustrate Cutkosky's rule, infrared divergence, and the singularity due to $m^2 \rightarrow 0$.

¹⁹ R. E. Cutkosky, J. Math. Phys. 1, 429 (1960).

by p' and one proton denoted by p . Inserting the states of these two particles and summing their spins, Eqs. (B1) becomes

$$\begin{aligned} i\langle | A_2^\dagger \int (2\pi)^4 \delta^4(p_1 + p_2 - p - p') \\ \times \frac{d^3 p'}{2E'} \frac{d^3 p}{2E} \frac{1}{(2\pi)^6} (\mathbf{p} + M)(\mathbf{p}' + m) A_2 | \lambda_2 \rangle \\ = i\langle | A_2^\dagger \int \frac{d^4 p'}{(2\pi)^4} [i(\mathbf{p} + M) 2\pi i \delta_+(p^2 - M^2)] \\ \times [i(\mathbf{p}' + m) 2\pi i \delta_+(p'^2 - m^2)] A_2 | \lambda_2 \rangle. \end{aligned} \quad (\text{B2})$$

Now except for the factor i in front of $\langle |$, the expression (B2) is exactly what one obtains by applying the Cutkosky rule to the usual Feynman rule for the two-photon-exchange diagram. The origin of i in front of $\langle |$ is that the usual Feynman rule refers to the S -matrix element which differs from the matrix element of A by a factor of i [see Eq. (A1)]. Since we are interested only in the interference terms between two matrix elements, only the relative phase between them enters into the problem and the factor of i above always get canceled out as long as we use the same phase convention for the two matrix elements.

In order to illustrate some of the interesting features of the two-photon-exchange mechanism and the use of the Cutkosky rule, let us consider an integration whose real and imaginary parts are known²⁰:

$$\begin{aligned} b = \int \frac{id^4 k}{(k^2 - 2p_1 \cdot k)(k^2 + 2p_2 \cdot k)[(k - q)^2 - \lambda^2](k^2 - \lambda^2)} \\ = -\frac{\pi^2}{sq^2} \ln \frac{-q^2}{\lambda^2} \left(\ln \frac{s}{m^2} - \pi i \right). \end{aligned} \quad (\text{B3})$$

This integration occurs in the two-photon-exchange diagram in the e - e scattering shown in Fig. 9. The answer is correct in the limit $s \gg m^2 \gg \lambda^2$ and $-q^2 \gg m^2$, where $s = (p_1 + p_2)^2$, $q^2 = (p_1 - p_3)^2$, $p_1^2 = p_3^2 = m^2$, and λ^2 is the fictitious mass of the photon for handling the infrared divergence.

Applying the Cutkosky rule, we can easily calculate the following integration:

$$\begin{aligned} b_{\text{cut}} = \int \frac{i(2\pi i)^2 \delta_+(k^2 - 2p_1 \cdot k) \delta_+(k^2 + 2p_2 \cdot k)}{[(k - q)^2 - \lambda^2](k^2 - \lambda^2)} d^4 k \\ = \frac{2\pi^3 i}{sq^2} \ln \frac{-q^2}{\lambda^2}. \end{aligned} \quad (\text{B4})$$

Comparing Eq. (B3) with Eq. (B4), we obtain

$$2i \text{Im} b = b_{\text{cut}}. \quad (\text{B5})$$

Equation (B3) is not easy to calculate, whereas Eq. (B4) is relatively easy. Hence the Cutkosky rule is just a quick way to obtain the imaginary part of a matrix element. Equations (B3)–(B5) give the correct sign and numerical factors in applying the rule.

This example also shows that in general the two-photon-exchange diagram has an infrared divergence in both the real and imaginary parts. The reason that we do not have an infrared divergence in the up-down asymmetry is that the infrared-divergent part is always proportional to the lowest Born diagram, which does not produce any up-down asymmetry. We also notice that the imaginary part is finite as $m^2 \rightarrow 0$, whereas the real part diverges logarithmically as $m^2 \rightarrow 0$. (Compare with Appendix D.)

APPENDIX C

In this appendix, we show explicitly that the infrared-divergent part of the matrix element is proportional to the lowest-order diagram and hence does not contribute to the up-down asymmetry. The matrix element for the two-photon-exchange diagram shown in Fig. 6(b) can be written as (ignoring numerical factors)

$$\begin{aligned} T_2 = \int \frac{d^4 k}{(2\pi)^4} \bar{u}(p_3) \gamma^\lambda \frac{\mathbf{p}_1 - \mathbf{k} + m}{k^2 - 2p_1 \cdot k} \gamma^\mu u(p_1) \bar{\Psi}^\alpha(p_f) \gamma_5 \pi_{\lambda\alpha}(q - k) \\ \times \frac{\mathbf{p}_2 + \mathbf{k} + M}{k^2 + 2p_2 \cdot k} \Gamma_\mu(k) u(p_2) \frac{1}{(q - k)^2 - \lambda^2} \frac{1}{k^2 - \lambda^2}. \end{aligned}$$

Since the infrared divergence occurs at $k \rightarrow 0$, the infrared-divergent part of M_2 can be obtained by letting all the k 's in the numerator and in the denominator $(q - k)^2 - \lambda^2$ be equal to zero. We also note that

$$(\mathbf{p}_1 + m) \gamma^\mu u(p_1) = 2p_1^\mu u(p_1), \quad \Gamma_\mu(k) \xrightarrow{k \rightarrow 0} \gamma_\mu,$$

and

$$(\mathbf{p}_2 + M) \gamma_\mu u(p_2) = 2p_{2\mu} u(p_2).$$

Hence the infrared-divergent part of M_2 is equal to

$$\begin{aligned} T_2^{\text{infrared}} = \bar{u}(p_3) \gamma^\lambda u(p_1) \bar{\Psi}^\alpha(p_f) \gamma_5 \pi_{\lambda\alpha}(q) u(p_2) (1/q^2) \\ \times 4(p_1 \cdot p_2) \int \frac{d^4 k}{(2\pi)^4} \frac{1}{(k^2 - 2p_1 \cdot k)(k^2 + 2p_2 \cdot k)(k^2 - \lambda^2)}, \end{aligned}$$

which is proportional to the lowest-order graph T_1 shown in Fig. 6(a).

Even though there is no infrared divergence in the up-down asymmetry, in practical calculations one has to be careful in choosing the coordinate system in order to avoid numerical difficulties near $k^2 \rightarrow 0$ (see Sec. IV and Appendix D).

²⁰ M. L. G. Redhead, Proc. Roy. Soc. (London) **A220**, 219 (1953); R. V. Polovin, Zh. Eksperim. i Teor. Fiz. **31**, 449 (1956) [Soviet Phys. JETP **4**, 385 (1957)]; Y. S. Tsai, Phys. Rev. **120**, 269 (1960), and unpublished.

APPENDIX D

In this appendix we show that no singularity will be induced by ignoring the mass of the electron in the two-photon-exchange contribution to the up-down asymmetry A_t . We have shown this explicitly in Sec. IV when the hadron intermediate state is a proton and the final state is N^* , via an $M1$ transition. Using gauge invariance, we show that this is true also for an arbitrary final and intermediate hadron state. When the mass of the electron is ignored, q'^2 vanishes when \mathbf{p}' is parallel to \mathbf{p}_3 [see Fig. 7(b)]. When \mathbf{p}' is almost parallel to \mathbf{p}_3 , q'^2 is proportional to θ'^2 , where θ' is the angle between \mathbf{p}_3 and \mathbf{p}' . The solid angle is proportional to θ' ; hence all we need to prove is that $L^{\nu\lambda}B_{\mu\nu\lambda}$ is proportional to θ' when \mathbf{p}_3 and \mathbf{p}' are almost parallel to each other and the mass of the electron is ignored. Let us choose the direction of $\mathbf{q}' = \mathbf{p}' - \mathbf{p}_3$ as the z axis, and both \mathbf{p}' and \mathbf{p}_3 are on the xz plane in the c.m. system. When the mass of the electron is ignored, we have

$$q'^2 \equiv (\mathbf{p}' - \mathbf{p}_3)^2 = q_0'^2 - q_z'^2 \approx -E'E_3\theta'^2. \quad (\text{D1})$$

Let us consider first the case when the masses of the final and the intermediate hadron states are not equal to each other, so that $q_0' \neq 0$. Then from Eq. (D1) we may write

$$q_\lambda' = (q_0', q_x', q_y', q_z') = q_0'(1, 0, 0, 1 + (E'E_3\theta'^2/2q_0'^2)). \quad (\text{D2})$$

Equation (D2) together with current conservation $q'^\lambda B_{\mu\nu\lambda} = 0$ yields

$$B_{\mu\nu 0} = B_{\mu\nu z}(1 + E'E_3\theta'^2/2q_0'^2). \quad (\text{D3})$$

In the same coordinate system, the four-vector p_3 (mass ignored) can be written as

$$p_{3\lambda} = E_3(1, \sin\theta_3, 0, \cos\theta_3),$$

where

$$\theta_3 = \theta' E'/Q'.$$

Hence

$$\begin{aligned} p_{3\lambda} B_{\mu\nu\lambda} &= E_3(B_{\mu\nu 0} - B_{\mu\nu z} \cos\theta_3 - \sin\theta_3 B_{\mu\nu x}) \\ &\approx -(E_3 E' \theta'/Q') B_{\mu\nu x} + O(\theta'^2). \end{aligned} \quad (\text{D4})$$

When the spin of the electron is ignored, the lepton trace $L^{\nu\lambda\mu}$ is equal to $8p_1^\nu p_3^\lambda p_1^\mu$ as shown in Eqs. (4.2) and (4.3). Hence $L^{\nu\lambda\mu} B_{\mu\nu\lambda} \propto \theta'$ as desired. Now suppose we restore the spin of the electron, but ignore its mass; we have from Eq. (4.2)

$$\begin{aligned} \frac{1}{2} L^{\nu\lambda\mu} &= \frac{1}{4} \text{Tr}(\not{p}_1 \gamma^\nu \not{p}_3 \gamma^\lambda \not{p}' \gamma^\mu) \equiv (\not{p}_1 \gamma^\nu \not{p}_3 \gamma^\lambda \not{p}' \gamma^\mu) \\ &= p'^\lambda (\gamma^\mu \not{p}_1 \gamma^\nu \not{p}_3) - g^{\lambda\mu} (\not{p}' \not{p}_1 \gamma^\nu \not{p}_3) + p_1^\lambda (\not{p}' \gamma^\mu \gamma^\nu \not{p}_3) \\ &\quad - g^{\lambda\nu} (\not{p}' \gamma^\mu \not{p}_1 \not{p}_3) + p_3^\lambda (\not{p}' \gamma^\mu \not{p}_1 \gamma^\nu). \end{aligned} \quad (\text{D5})$$

Using the previous arguments, the terms proportional to p_3^λ and $p'^\lambda = p_3^\lambda + q'^\lambda$ in Eq. (D5) yield terms proportional to θ' in $L^{\nu\lambda\mu} B_{\nu\lambda\mu}$. We notice that in the rest of the terms in Eq. (D5), \not{p}_3 and \not{p}' are next to each other inside the trace. When \not{p}_3 and \not{p}' are parallel to each other, these terms are equal to zero separately if the mass of the electron is ignored. Hence we have proven that neglecting the mass of the electron does not cause any singularity in the imaginary part of the two-photon-exchange diagram for arbitrary final and intermediate states of hadrons provided that they have different invariant masses.

We next consider the case in which the virtual photon is coupled to the hadrons with identical invariant masses such as $\gamma p p$ or $\gamma N^* N^*$ couplings. The vertex labeled μ with momentum transfer k in Fig. 6(b) is such an example. In this case the energy transfer is zero in the c.m. system, and hence Eqs. (D2) and (D3) are meaningless. We notice that in this case the vanishing of q'^2 in the forward scattering is independent of the mass of the electron, as can be seen from Eq. (4.12) where M^2 and M_f^2 are now equal to each other. We also notice that in this case the kinematics is such that in order to have a vanishing q'^2 , all four components of q' must vanish, which is precisely the infrared limit. Since we know there is no infrared divergence for the up-down asymmetry independent of the value of the mass of the electron, we conclude that the mass of the electron can be ignored in this case as well. In contrast to the previous case, the nonexistence of the infrared divergence depends critically upon the fact that there are odd numbers of γ_5 in $B_{\mu\nu\lambda}$; hence it is true only for the asymmetry, but not true in general for the imaginary part of the two-photon-exchange diagram (see Appendices B and C).

This observation not only enables us to ignore the electron mass in this kind of calculation but also tells us that there will be no terms such as $\alpha \ln(s/m^2)$ or $\alpha \ln(-q^2/m^2)$ in the asymmetry A_t . It should be emphasized however that in the actual numerical integration with respect to the solid angle of \mathbf{p}' , even though we have proven that the singularities due to the two-photon propagators are canceled by the zeros in the numerator, one has to choose coordinate systems properly—otherwise the integrand is too singular to perform the numerical integration even if the electron mass is not ignored. In Sec. IV, we have chosen the z axis to be along \mathbf{p}_3 and \mathbf{p}' is almost parallel to \mathbf{p}_3 , and along \mathbf{p}_1 when \mathbf{p}' is almost parallel to \mathbf{p}_1 . We have found that no trouble arises even if the mass of the electron is ignored.